UNIVERSIDADE DE LISBOA
FACULDADE DE CIÊNCIAS
DEPARTAMENTO DE BIOLOGIA VEGETAL

The impact of *Lama2*-deficiency on cell cycle regulation and survival

Catarina Elisa Mineiro de Melo

Mestrado em Biologia Molecular e Genética

Dissertação orientada por:
Doutora Ana Rita Carlos

2021

Acknowledgements

This was a challenging year but, at the same time, very rewarding. I had the opportunity to meet and work with amazing people who made the whole experience more enjoyable.

First, I would like to thank the person who has become one of the main reasons for having enjoyed this experience so much, my advisor, Rita Carlos. It was a pleasure sharing this year's work with you. Despite all the setbacks, you always looked at things positively and always found a way to overcome them. I want to thank you for pressuring me with the writing and for the amazing review to improve this thesis. For all the patience, the immense availability, and the effort to make me a more independent and confident person in my abilities. Thank you for always treating as an equal and for teaching me so much. I wish you all the best and success for your future.

I want to thank Sólveig Thorsteinsdóttir, for all the suggestions revising my thesis and for allowing me to be part of this amazing group, full of people always ready to help. I also want to thank Gabriela Rodrigues, Rita Zilhão and Antonio Cordero for the review. I'm so grateful for all the help.

I also would like to thank Susana Martins, for being my second teacher and a pro reviewer. You helped me so much across this journey, including knowledge related to the different techniques I used for this work. I'm grateful to have met you, for all the moments of laughter and friendship, for all the times you helped me in the lab, for whatever reason, and for making me believe that everything would go well. Thank you also for helping me concentrate while writing the thesis, whenever I got distracted ("escreve, escreve"). I wish you all the success on this journey and I know you will rock.

I also would like to thank both Susana and Rita, responsible to sacrifice the mice used in this study. Since the beginning, and for a long time, it was just the three of us in our little DEM girls' group.

Also, I would like to thank Bérénice Saget for the help with immunofluorescence and the ko clone generation. Your time in the lab was brief, but it was a pleasure to meet you and work with you. Thanks to you, I was able to practice my English and feel less embarrassed about speaking it.

Then, I would like to thank Marta Palma, for all the support with everything needed in the lab, and Joaquim Tapisso for assisting in the care of the mice in the animal house.

I also would like to thank the other members of the group, Luis for the support in microscopy, Inês Fonseca for the energy and fun moments you provided and the company on long afternoons plating cells (and our successful stand-up duo), Vanessa Ribeiro for being such an inspiring and fun person (Las chicas cantantes, together with Susana, would be a success for Christmas and various festivities 😜), Pedro Santos, Rita Soares and Hugo Luiz. Thank you for all the fun lunches and the moments we've shared.

I want to thank the support given to this project, by Association Française contre le Myopathies (AFM) Téléthon (contract no. 23049), L'Oréal Portugal Medals of Honor for Women in Science 2019, and Fundação para a Ciência e Tecnologia Project (Ref. PTDC/BTM-ORG/1383/2020) and Unit Funding (Ref. UIDB/00329/2020).

Last but not least, I would like to thank my family and friends. A special thank you to my parents for always making all the efforts for me to have a happy and successful future, and for supporting me unconditionally. Thank you for believing and encouraging me and for all the love and everything you taught me. I also want to thank all my friends that I had the pleasure to meet and that made me the person I am today. It is amazing to see how much we have grown over these years. Thank you for always being there, for all your motivation and for making my days happier.

Thank you for everything.

Abstract

Laminin α2 chain-deficient congenital muscular dystrophy (LAMA2-CMD) is caused by recessive mutations in the *LAMA2* gene. This neuromuscular disease is diagnosed at birth or within the first few months of life and is characterized by hypotonia and severe muscle weakness. Using the dyW mouse model of LAMA2-CMD, previous studies by the host laboratory showed that the onset of this muscular dystrophy occurs *in utero*, more specifically between embryonic days 17.5 and 18.5 (E17.5-E18.5), where it is observed a reduction in the size of muscle fibers and lower expression of the myogenic factors Pax7 and Myogenin. These alterations may be related to changes in cell cycle and cell survival regulation, as revealed by the overactivation of the transcription factor STAT3 and increased expression of the respective target gene *Pim1*. To investigate how *Lama2*-deficiency impacts on cell cycle regulation and survival, we used RT-qPCR and Western Blot to analyze the expression of genes and proteins involved in different cell fate pathways, comparing epaxial muscles of wildtype (wt) and dyW mice at E17.5 and E18.5. We also generated C2C12 myoblast cell lines deficient for *Lama2* and for both *Lama2* and *p53*, a master transcription regulator of cell cycle and survival. Using these *in vitro* models, pathways linked to proliferation/cell cycle were analyzed by RT-qPCR, immunofluorescence and Resazurin assay. Our results suggest a difference in genes linked to cell cycle regulation, proliferation, autophagy and senescence. C2C12 *Lama2* knockouts revealed a decrease in proliferation, possibly explained by cell cycle arrest at G1/G0 phase, which was partially rescued by the co-deletion of Lama2 and p53. This work highlighted alterations in terms of cell fate regulation, involved in LAMA-CMD onset, and resulted in the generation of an *in vitro* model, both important to gain further mechanistic insights about this disorder and to develop efficient therapies.

Keywords: Laminin α2 chain-deficient congenital muscular dystrophy, Skeletal muscle, Cell cycle and survival, CRISPR, Proliferation.

Resumo alargado

A distrofia muscular congénita deficiente na cadeia α2 da laminina (LAMA2-CMD) é causada por mutações recessivas no gene *LAMA2*. Esta doença neuromuscular é diagnosticada à nascença ou nos primeiros meses de vida e é caracterizada por hipotonia e fraqueza muscular grave. Utilizando o modelo de ratinho dyW para LAMA2-CMD, estudos anteriores do laboratório revelaram que o aparecimento desta distrofia muscular ocorre *in utero*, mais especificamente entre os estádios fetais 17.5 e 18.5 (E17.5-E18.5), sendo possível observar uma redução do tamanho das fibras musculares e uma menor expressão dos fatores miogénicos Pax7 e Miogenina. Estas alterações podem estar relacionadas com mudanças na regulação do ciclo celular e sobrevivência, como revelado pela sobreativação do fator de transcrição STAT3 e aumento de expressão do respetivo gene-alvo *Pim1*. No entanto, ainda não é claro quais as vias alteradas no início da LAMA2-CMD. Uma melhor compreensão das alterações no contexto da LAMA2-CMD é imperativa para o desenvolvimento de novas terapias. Este projeto visa analisar os mecanismos de destino celular que sofrem alterações durante o início desta doença e testar se estes podem ser contrariados pela supressão do fator de transcrição p53. Para isso, foram realizadas as seguintes tarefas:

- → Análise de vias envolvidas na regulação do ciclo celular e sobrevivência celular (incluindo quiescência/proliferação, apoptose, senescência e autofagia) que podem ser alteradas na ausência de *Lama2 in vivo*, comparando os músculos epaxiais de ratinho selvagens (wt) com ratinhos dyW em E17.5 e E18.5. Assim, será possível ter uma melhor compreensão dos mecanismos que desencadeiam o aparecimento desta condição, de modo a desenvolver novas terapias para o tratamento desta distrofia
- → Estabelecer e testar uma linha celular C2C12 mutante em *Lama2*, utilizando a tecnologia CRISPR/Cas9, para estudar a deficiência de laminina α2 *in vitro*.
- → Testar se a deleção de p53 na ausência de *Lama2* melhora o fenótipo LAMA2-CMD *in vitro*.

Para avaliar o impacto de alterações no ciclo celular e da sobrevivência no início da LAMA2-CMD, foram analisadas diferentes vias *in vivo* em ratinhos dyW e *in vitro*, utilizando células C2C12 com mutação em *Lama2*, recorrendo a várias técnicas de biologia celular e molecular, incluindo Real Time-qPCR (RT-qPCR), Western Blot, imunofluorescência, citometria de fluxo e análise de proliferação. A análise da expressão dos genes ligados à proliferação/quiescência nos músculos fetais revelou um aumento significativo na expressão de *Cdkn1a* (p21) e *Cdkn1c* (p57) em E17.5 e um aumento de expressão de *Cdkn1a* em E18.5, embora não significativo (p= 0,1263), sugerindo uma diminuição da proliferação e indução da paragem do ciclo celular. Em concordância, a deteção de histona H3 fosforilada por imunofluorescência e a análise da proliferação celular com Resazurina demonstraram uma redução da proliferação das células deficientes em *Lama2* comparativamente com as células saudáveis (Wt). A análise complementar *in vitro*, feita por citometria de fluxo, mostrou que a diminuição da proliferação se poderá dever à paragem do ciclo celular, uma vez que os resultados demonstraram um aumento de células em fase G1/G0 quando comparadas com Wt, sugerindo que a deficiência em *Lama2* poderá levar à paragem neste ciclo celular.

Em condições de homeostase, o p53 está constantemente a ser degradado, no entanto, após algum tipo de stress, o p53 é estabilizado e ativado, regulando diferentes vias de sinalização. Estudos anteriores revelaram que este fator de transcrição, conhecido por desencadear a paragem do ciclo celular (por exemplo, através da indução da expressão *Cdkn1a*/p21, levando à paragem na fase G1), se encontrava induzido e acumulado nos núcleos das células miogénicas LAMA2-CMD humanas e em ratinhos *Lama2*$^{-/-}$, resultado que está de acordo com o aumento dos níveis de expressão de p53 no músculo esquelético fetal em E18.5, detetados no presente trabalho. Assim, sugere-se que uma diminuição da expressão de p53 poderia recuperar defeitos proliferativos observados em condições de deficiência de *Lama2*. O papel deste fator de transcrição neste contexto foi avaliado pela redução da

expressão de *p53* combinado com mutações no gene *Lama2* (dko), em células C2C12. Utilizando o ensaio de proliferação de Resazurina, foi possível verificar uma melhoria na proliferação celular dos clones dko, passando a ser semelhante ao Wt.

A análise de genes envolvidos na regulação da autofagia *in vivo* revelou que a expressão de *Lamp2a* em E18.5 era semelhante para dyW e wt, mas a expressão de *Atg7* revelou-se significativamente aumentada, demonstrando uma possível ativação da autofagia. Embora a apoptose seja uma marca típica em várias distrofias musculares, incluindo LAMA2-CMD, este processo não é aumentado nos músculos durante o desenvolvimento embrionário. Estes resultados estão de acordo com os nossos, uma vez que os valores de expressão de *Bax* e *Bcl2* não foram significativamente alterados em comparação com os dos ratinhos wt. A apoptose só é significativa em contexto pós-natal, aquando da acumulação considerável de danos. Assim, é provável que o aumento da apoptose não seja a razão para a diminuição das células estaminais musculares e redução do tamanho da miofibras, de acordo com os resultados anteriores. Embora haja uma estreita relação entre autofagia e apoptose, a autofagia pode agir conjuntamente com a apoptose e induzir a morte celular ou, por outro lado, reprimi-la. Os resultados não foram conclusivos sobre esta ligação. A senescência caracteriza-se pela expressão do fenótipo secretor associado à senescência (SASPs), que incluem a secreção de várias citocinas inflamatórias e interleucinas. Os membros da família CCL podem aparecer regulados em células senescentes. Em concordância, o gene Ccl7, que codifica para o ligando 7 da quimiocina (motivo C-C) (CcL7), estava significativamente aumentado em ratinhos dyW, sugerindo que a senescência pode ser predominante neste genótipo. *Il-6ra*, que codifica para a cadeia alfa do recetor de Il-6, é um recetor ao qual se liga Il-6, desencadeando diferentes vias de transdução de sinal e transcrição de diversas citocinas que medeiam respostas inflamatórias e senescência. Para além disso, está envolvido na ativação da via JAK-STAT3, que pode levar tanto à proliferação dos mioblastos e prevenção de diferenciação prematura com à diferenciação miogénica. A expressão *Il-6ra* estava aumentada em ratinhos dyW em E17.5 (p=0,0943), mas a expressão em E18.5 foi semelhante para ambos os genótipos. Em consonância, a fosforilação de STAT3 em dyW revelou uma tendência a estar aumentada em comparação com o wt, embora não fosse significativo, em concordância com resultados anteriormente obtidos. Assim, Il-6ra poderá contribuir para uma maior ativação do JAK-STAT. A sobreactivação de JAK-STAT3 tem sido demonstrada como sendo característica das MuSCs envelhecidas que apresentam uma regeneração muscular deficiente e, para além disso, foi também sugerido o seu envolvimento na promoção das divisões assimétricas das MuSCs. Portanto, existe a possibilidade da laminina-211 estar envolvida no controlo da ativação de STAT3, através da ligação e ação da integrina α7β1 (integrina esta que se liga a *Lama2*), e impeça a sobreactivação da via JAK-STAT3, favorecendo assim as divisões simétricas para manter a população de MuSCs Pax7 positivas. Para além disso, a sobreactivação JAK-STAT3 poderá também promover a expressão myoD, que induz a paragem do ciclo celular.

Os nossos resultados de RT-qPCR *in vivo* demonstram um aumento da expressão do *Cdkn1a*, aliada a uma deficiência na proliferação, que juntos podem explicar o número reduzido de MuSCs, resultando em menos células miogénicas. Embora a ligação entre LAMA2-CMD e senescência não tenha sido estabelecida, estudos apontam para uma exacerbação da distrofia muscular de Duchenne provocada pela senescência crónica e que a inibição da senescência resultaria em melhorias da doença. Com a expressão aumentada Ccl7 e Il-6ra, seria esperado que ocorresse um aumento da inflamação nos músculos dyW. No entanto, Nunes et al. demonstrou que tanto a inflamação como da fibrose não apareciam aumentadas em E17.5 ou PN2.

De um modo geral, a paragem do ciclo celular parece estar aumentada, quer pelo aumento da expressão de *Cdkn1a* e *Cdkn1c*, quer pela expressão reduzida do marcador de proliferação *Mki67*, sendo esta paragem do ciclo celular característica necessária para a ocorrência de outros mecanismos, especialmente a quiescência, senescência e a apoptose. Isto é também suportado pelos dados obtidos *in vitro*. Embora não houvesse diferença nos genes relacionados com a apoptose, um dos dois genes

analisados e relacionado com a senescência – Ccl7 –, apresentava um aumento de expressão. O aumento de expressão de *Atg7*, gene envolvido na autofagia, pode revelar um esforço das células para manter as necessidades metabólicas e, possivelmente, controlar níveis aumentados de espécies reativas de oxigénio (ROS), característica dos pacientes LAMA2-CMD. Assim, estes dados apontam para a hipótese de que o aumento da autofagia ocorre como oposição ao aumento de ROS, conduzindo assim à diminuição da atividade metabólica e consequente diminuição da proliferação, quer pela entrada em quiescência, quer pela senescência.

Embora atualmente não exista cura ou tratamentos eficientes para LAMA2-CMD, diversos estudos com diferentes terapias experimentais encontram-se em curso. Assim, este trabalho permitiu enriquecer o conhecimento sobre como a ausência de *Lama2* poderá impactar e alterar os mecanismos envolvidos no destino celular no início da LAMA2-CMD, mais propriamente durante o desenvolvimento fetal do ratinho. Sendo esta a distrofia muscular congénita mais comum, uma melhor compreensão dos mecanismos que desencadeiam o aparecimento desta condição é crucial para desenvolver abordagens terapêuticas que possam prolongar o tempo de vida e aumentar o bem-estar dos pacientes.

Palavras-chave: Distrofia muscular congénita deficiente na cadeia α2 da laminina, Músculo esquelético, Ciclo celular e sobrevivência, CRISPR, Proliferação.

Contents

List of figures and tables

List of abbreviations and symbols

°C – Degrees Celsius
Arbp0 – Acidic ribosomal phosphoprotein PO
ATG – Autophagy-related
BM – Basement membrane
bp – Base-pair
BSA – Bovine Serum Albumin
CAK – CDK-activating kinases
CDK – Cyclin-dependent kinases
cDNA – Complementary DNA
CKI – CDK-inhibitor
Ct – Cycle threshold
DAPI – 4′,6-diamidino-2-phenylindole
dko – Double knockout
DMEM – Dulbecco's Modified Eagle's Medium
DTT – Dithiothreitol
E0.5 – Embryonic stage 0.5
E11.5 – Embryonic stage 11.5
E14.5 – Embryonic stage 14.5
E15.5 – Embryonic stage 15.5
E16.5 – Embryonic stage 16.5
E17.5 – Embryonic stage 17.5
E18.5 – Embryonic stage 18.5
E8.5 – Embryonic stage 8.5
ECM – Extracellular matrix
FAP – Fibro/adipogenic phenotype
FBS – Fetal Bovine Serum
gRNA – Guide RNA
h – Hour
HRP – Horse Radish Peroxidase
HSPG – Heparan sulfate proteoglycan
IFN – Interferon
IL – Interleukin
Il-6ra – Il-6 receptor alpha chain
JAK-STAT – Janus kinase signal transducer and activator of transcription
kDa – Kilodalton
ko – Knockout
Lama2 ko – *Lama2* knockout C2C12 cells
Lama2/p53 ko – *Lama2* and *p53* knockout C2C12 cells
LAMA2-CMD – LAMA2-deficient congenital muscular dystrophy
LB – Lysogeny Broth
LE – Laminin-type epidermal growth factor-like domain
LG – Laminin G-like domain
LN – Laminin N-terminal domain
M – Molar
mg – Milligram
mg – milligram
min – Minutes
mL – Milliliter
MRF – Myogenic regulatory factors
mRNA – Messenger RNA
mTOR – Mechanistic target of rapamycin
MuSC – Muscle stem cell
nm – Nanometer
p53 ko – *p53* knockout C2C12 cells
PAM – Protospacer adjacent motif
PBS – Phosphate-Buffered Saline
PCR – Polymerase chain reaction
pH3 – Phospho-Histone 3
PI – Propidium iodide
PN2 – Postnatal day 2
pSTAT3 Tyr 705 – STAT3 phosphorylated at tyrosine 705
PVDF – Polyvinylidene Fluoride
ROS – Reactive oxygen species
rpm – Rotations per minute
RT – Room temperature
RT-qPCR – Real time qPCR
SASP – Senescence-associated secretory phenotype
SDS-PAGE – Sodium Dodecyl Sulphate-Polyacrylamide Gel Electrophoresis
sec – Seconds
TBST – Tris Buffered Saline 0,1% Tween
WB – Western Blot
Wt – Wiltype (C2C12 cells)
wt – Wiltype (mice)
µL – Microliter

Chapter 1 Introduction

The extracellular matrix (ECM) is a non-cellular component present in all tissues, forming a physical scaffold for cells[1]. It confers not only physical support but also biochemical and biomechanical cues, vital for tissue morphogenesis, differentiation and homeostasis. Thus, by interacting with cell-surface receptors, the ECM allows signal transductions and regulates gene expression, which controls several fundamental cellular pathways including proliferation, polarization, migration, differentiation, survival and apoptosis[2]. In addition, it plays an active role in connective tissue remodeling and repair[3].

ECM composition includes a combination of proteoglycans and fibrous glycoproteins, which vary according to the functional needs of each tissue and confers different biophysical, biochemical and topological properties, according to their function[4]. Some of these properties include tensile and compressive strength, elasticity and also serves as a buffer that protects the tissues by maintaining extracellular homeostasis and water retention[1]. This tissue-specific and highly dynamic structure exists in two major forms: interstitial ECM and the basement membrane (BM)[2].

Interstitial ECMs are the matrix of connective tissue. Mainly formed by collagens, which are usually secreted by fibroblasts, they provide tensile strength, regulate cell adhesion, mediate migration and tissue development[4]. Other crucial components include elastin, fibronectin and tenascin. The proteoglycans, also part of the interstitial matrices, confer hydration and protect the tissue by opposing compressional forces[5].

BMs are specialized types of ECM that surrounds certain animal tissues[6]. BMs are in close contact with epithelial and endothelial cells and surround, for example, the different types of muscle cells, adipocytes, neurons and Schwann cells, present in peripheral nerves, separating (or isolating) these from the surrounding connective tissue[7]. Fundamentally, BMs are composed of a network of proteins, essential for the structural support of the cell layers to which they adhere, and are therefore crucial for the maintenance and differentiation of several animal tissues. BMs stabilize cells and tissues by providing solid phase cell adhesion substrates, linking the ECM to the cytoskeleton[8]. BMs are deposited from the earliest stages of embryonic development, and their main components include laminins, type IV collagens, nidogens, and the heparan sulfate proteoglycan (HSPG) perlecan, where the three first components are thought to constitute the central BM scaffolding[9] (Figure 1.1 A).

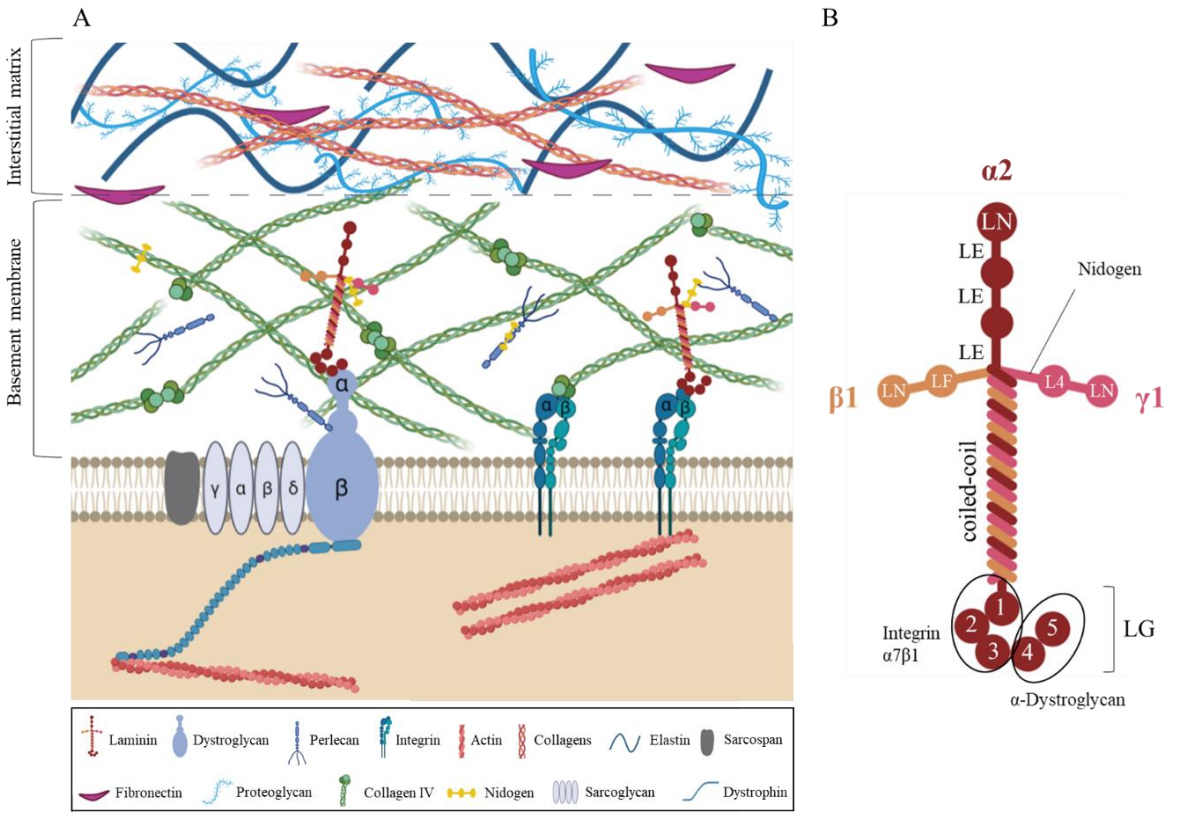

Figure 1.1 Extracellular Matrix composition and laminin-211 structure. (A) Interstitial matrix includes collagens, elastin, fibronectin and proteoglycans. As for BM, the main components are laminins, collagens (collagen IV), nidogens and perlecans. These components communicate with the cells via transmembrane receptors (dystroglycan, integrins and syndecans). In the skeletal muscle, dystrophin-glycoprotein complex (dystroglycan, sarcoglycan, sarcospan) links the laminins to the actin fillaments through dystrophin. (B) laminin-211 is composed by α, β and γ chains organized in a coiled coil. α chain long arm ends in a C-terminal globular domain with a combination of five laminin G-like (LG) domains. LG1-3 binds to integrins (specially Integrin α7β1), and LG-4-5 binds to α-dystroglycan domain. The α, β and γ short arms, involved in laminin assembly, have a laminin N-terminal (LN) domain followed by tandem repeats of laminin-type epidermal growth factor-like (LE) domains. Adapted from [10].

1.1 Structure and function of basement membrane components

Laminins are a family of cell adhesion glycoproteins that form a large heterotrimeric structure, composed of α, β and γ subunits in a cruciform shape (Figure 1.1 B). They contain a α-helical coiled coil long arm combining all the subunits and the three short arms from the respective subunit, and C-terminal globular domain of the α chain ends in a combination of five laminin G-like (LG) domains. The short arms of each subunits have different lengths but possess similar structures: a laminin N-terminal (LN) domain followed by tandem repeats composed by laminin-type epidermal growth factor-like (LE) domains. LN domains are crucial for laminin self-assembly into a scaffold[11]. So far, several isoforms of each subunit have been identified (five α subunits, four β subunits and three γ subunits) and their combination results in 18 different laminin isoforms[12]. Although there is a sequence similarity between subunits, many of them display tissue-specific expression and function. Depending on the presence or absence of the short arm domain, laminins can self-assemble through the LN domains of the respective subunits, as previously mentioned[8]. For that reason, some laminins that have a reduced short arm lack the ability to self-assemble, including the laminin-α3A or laminin-α4 isoforms. The general role of laminins is to create a structure that (1) links the ECM to the cell surface and (2) connects and stabilize the other components of BMs[8].

Similar to laminins, collagen type IV is able to self-assemble and plays a significant role in cell adhesion, migration, growth and differentiation. Collagen IV degradation may occur under physiological and pathological conditions, and the resulting protein fragments act during angiogenesis,

tissue remodeling and cancer progression[13]. Nidogens are thought to play an important role in BM formation by bridging the laminin and collagen IV networks and interact with other components of BMs, thereby promoting a proper assembly of this structure[14].

As previously indicated, BMs are present around muscle cells, their composition being specific for each type of muscle. Vertebrates have three different types of muscles: smooth muscle, cardiac muscle and skeletal muscle. Smooth and cardiac muscles are controlled by the autonomous nervous system, thus having involuntary contraction, in contrast to the contraction of skeletal muscles which is voluntary, through the action of motor neurons. Skeletal muscle is composed of elongated multinucleated cells known as muscle fibers or myofibers, that are arranged parallel to each other. Each muscle fiber has numerous myofibrils, specialized structures composed by different proteins, including actin and myosin, that are organized in contractile units called sarcomeres, and which are vital for muscle contraction to occur. The organization in sarcomeres gives rise to the striated pattern characteristic of skeletal and cardiac muscles. While muscular contraction in skeletal muscle is triggered and controlled by motor nerves, in cardiac muscle the contraction of sarcomeres is modulated by the autonomous nervous system[15].

In skeletal muscle, the BM surrounds each myofiber and provides the elasticity so that the sarcolemma (muscle cell membrane) supports the mechanical stress of repeated muscular contractions. All the β- and the γ-laminin chains expressed in the skeletal muscle have the LN domains, so the polymerization ability only depends on the presence or absence of short α-chain and on the N-terminal end of the long α subunit[8].

The main laminin isoform in the skeletal muscle BM is laminin-211 (α2, β1 and γ1 subunits). The interaction between laminin-211 and the receptors integrin (especially integrin α7β1) and dystroglycan, present on the muscle cell surface, links the BM and the actin cytoskeleton of the myofiber. This important connection guarantees the normal functioning of skeletal muscles, since it maintains the assembly of the sarcolemmal BM[8,9] and protects the myofibers from damage caused by their contraction[16].

1.2 LAMA2 Congenital Muscle Dystrophy (LAMA2-CMD)

In skeletal muscle, the BM is crucial to maintain muscle integrity and also plays a role in regeneration[17]. The importance of the BM, and the ECM in general, is further demonstrated by the existence of several genetic diseases that result from mutations in the matrisome – a set of genes encoding ECM and ECM-associated proteins – leading to problems in terms of ECM structure assembly and function[3]. So far, 105 mutations in matrisome genes have been shown to cause various human disorders[3]. Some of these diseases, caused directly by mutations in genes coding ECM components or transmembrane ECM receptors, include Osteogenesis Imperfecta (OI), chondrodysplasias, Ehlers–Danlos syndromes (EDS), epidermolysis bullosa, Alport syndrome, Pierson syndrome and variety of muscular dystrophies.

Muscular dystrophies are a group of inherited disorders that reflect the consequences of ECM disruption, caused by different mutations in genes encoding ECM components and their effectors. These disorders are characterized by progressive muscle weakness and muscle wasting, caused by the incapacity of the myofibers to support the mechanical effort of contractions, thus leading to cell membrane rupture and muscle damage. Initially, muscles are able to regenerate but owing to damage accumulation, cells are no longer able to regenerate efficiently and die, creating room for adipocytes to infiltrate and replace the dead muscle cells[17].

Some examples of muscular dystrophies include LAMA2-deficient congenital muscular dystrophy (LAMA2-CMD), Ulrich congenital muscular dystrophy, Bethlem myopathy, Duchenne Muscular Dystrophy, Becker muscular dystrophy, Waker-Warburg syndrome and Fukuyama muscular dystrophy[3,18].

In this thesis, our focus is on LAMA2-CMD. This neuromuscular disease is triggered by autosomal recessive mutations in the *LAMA2* gene, coding for the α2 chain of laminins 211 and 221. While laminin-211 is the main isoform present in BM surrounding the myofibers, laminin-221 is mostly localized in neuromuscular junctions[19]. The reduction or absence of laminin-211 compromises ECM structure, exposing myofibers to constant stress and, consequently, cell damage, which causes muscle wasting, chronic inflammation and fibrosis. Apart from that, there is a deregulation of several cellular mechanisms, including increased apoptosis, as well as proteasome and autophagic overactivation[19,20].

In order to compensate for the absence of *Lama2* and prevent myofibers breakdown, cells increase *Lama4* and *Lama5* expression[21]. In the case of increased *Lama4* expression, this promotes the formation of laminin-411. However, laminin α4 chain is not able to self-assemble and polymerize with other BM components and does not bind to α-dystroglycan and integrin α7β1. Laminin α5 chain, which forms laminin-511, despite polymerizing properly, binds weekly to α-dystroglycan[8,23]. So, these two chains fail to compensate for *Lama2* deficiency and cannot restore BM assembly.

Despite being a rare disease, LAMA2-CMD is the most common congenital muscular dystrophy in Europe, corresponding to 37.4% of the cases. The severity of this disease depends on the degree of α2 chain deficiency[8]. Most *LAMA2* mutations correspond to nonsense mutations that results in a truncated form of the chain, a mutation that causes total deficiency of this subunit and induces a severe phenotype. Milder forms of LAMA2-CMD are normally missense mutations that show a decreased expression of *LAMA2*[8,23]. Patients with this disorder show several symptoms, such as delayed motor development, severe hypotonia, joint contractures, scoliosis and general muscle weakness, which prevents patients from being able to sit unsupported and be able to ambulate[8,24,25]. In addition to the effects in skeletal muscle, absence of *LAMA2* also impacts the peripheral and central nervous systems. In some patients, this mutation is shown to change white mater density and affect nerve conduction, due to myelination failure, which may lead to seizures or moderate mental retardation. Heart defects can also occur[8,26].

As a congenital dystrophy, patients often suffer from muscle weakness at birth or the early months of life and often die by the second decade of life due to muscle wasting and respiratory infection and failure[8]. Currently, LAMA2-CMD has no cure or effective treatments[27].

Several mouse models can be used to study the impact of *LAMA2* mutations, including the dyW, dy3K and dy2J mouse models[24,28]. The dyW mouse model of LAMA2-CMD, a mouse strain that expresses small amounts of an unstable truncated form of laminin α2 chain[29], is the most commonly used mouse model of LAMA2-CMD. Mice with this mutation display a severe phenotype and normally die 5–12 weeks after birth[30]. They are characterized by general muscle atrophy and degeneration, hindlimb paralysis, reduced locomotor activity, apoptosis, inflammation, fibrosis and peripheral neuropathy[31].

Even though events such as fibrosis and inflammation have been well characterized in the context of LAMA2-CMD, the mechanisms that trigger the onset of this pathology have not yet been described. Using the dyW mouse strain, the host laboratory has shown that the onset of this disease in mice occurs between embryonic stages 17.5 (E17.5) and E18.5 and are characterized by a reduction in myofiber size and a decrease in the number of muscle stem cells (MuSCs) and myoblasts[19], suggesting a potential impact in the formation of skeletal muscle tissue, a process termed myogenesis. Here we address the hypothesis that the dyW phenotype is associated with impaired cell proliferation, differentiation or survival of MuSCs and/or myoblasts.

1.3 Myogenesis in health and disease

Under normal physiological conditions, muscle development occurs throughout embryonic and fetal development. Skeletal muscle cells originate from embryonic structures known as somites, a structure that already possesses a BM matrix since early stages, containing laminins 111 and 511[19]. The

somites are spherical structures which mature to form four different compartments, including the dermomyotome[15]. This epithelial dermomyotome is composed of multipotent progenitor cells that will generate muscle progenitors, also called MuSCs[32]. The maintenance of the uncommitted and proliferative state of dermomyotomal cells allows dermomyotome growth, which occurs due to the expression of Pax3 and Pax7 transcription factors. Pax3 and Pax7 are uncommitted MuSC markers that mark the myogenic potential of dermomyotome cells[2,15].

The myogenic program is induced by the myogenic regulatory factors (MRFs), which comprise a family of transcription factors expressed in the skeletal muscle lineage, that activate cell commitment - Myf5, MyoD, Mrf4 – and lead to myogenic differentiation – Myogenin[33]. At E8.5, skeletal muscle development starts when some Pax3- and/or Pax7-positive MuSCs at the dermomyotome edge activate Myf5 and/or Mrf4 and delaminate to form the myotome[19]. These dermomyotome cells migrate to the myotomal space as committed myoblasts, then activate Myogenin and differentiate to form the first myocytes of the myotome[2]. Eventually, the dermomyotome de-epithelializes, leading to the release of proliferative MuSCs into the myotome, which are then referred as embryonic MuSCs[15].

Myoblasts continue to enter the myotome, activating a set of MRFs specific for each stage and hence contribute to myotome growth. The BM surrounding the dermomyotome cells, composed by assembled laminin 111 and 511, collagen type IV, perlecan and nidogen, is crucial to promote dermomyotome symmetric cell divisions and to maintain the undifferentiated state of myogenic progenitors, which prevents inappropriate differentiation[2,34]. Laminin-111, present since somite formation, is fundamental to guarantee the assembly of laminin-511 at the myotome/sclerotome border, and these two laminins work together to restrain myogenic cells in the myotome[34,35].

When in the myotome, if the markers of terminal specification Myf5 and/or MyoD are activated, the MuSCs differentiate into myoblasts, followed by the expression of Myogenin, which leads to myocyte differentiation[36]. Otherwise, MuSCs maintain the proliferative state, in order to form a pool of MuSCs[15]. Some of these cells will later differentiate during development and others will form a niche of quiescent MuSCs, already in the postnatal and adult phase, which will be important for muscle growth and regeneration[36].

Between E11.5 and E14.5, primary myogenesis is initiated in the mouse. In the trunk, the elongated myocytes start to fuse with each other and/or with the differentiated myoblasts to form the multinucleated primary myotubes which set the trunk muscle pattern[19]. At E14.5, these primary myotubes get attached to tendons and are innervated by motor neurons. During secondary myogenesis, from E14.5 until birth, the pool of embryonic MuSCs that remained uncommitted start a second wave of differentiation, forming the secondary myoblasts. The myotubes formed in the primary myogenesis form the basic muscle pattern and secondary myoblasts fuse close to the innervation site to form the secondary (fetal) myotubes[19,37]. Consequently, fetal skeletal muscle growth occurs by the addition of new myotubes surrounding the pre-existing primary myotubes and the secondary myoblasts also fuse to the primary myofibers, increasing their size[19] (Figure 1.2).

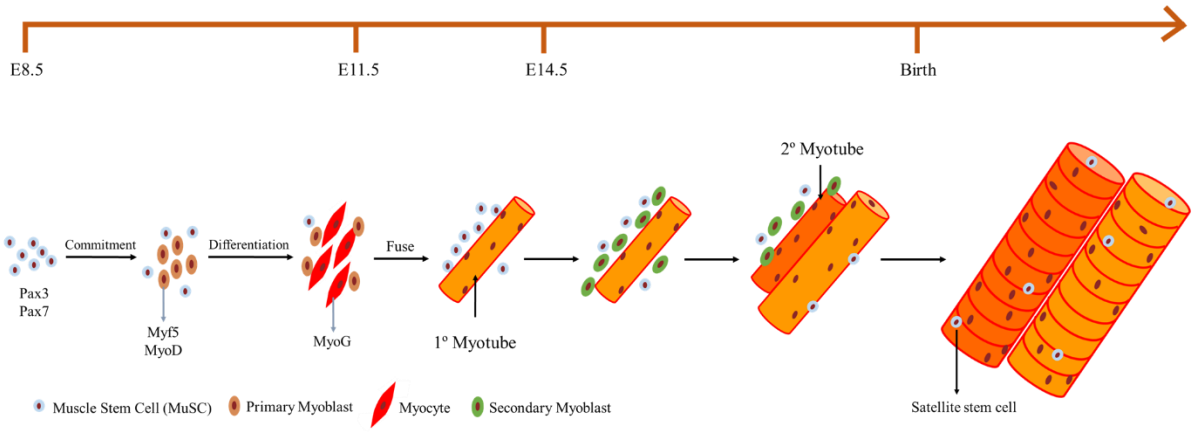

Figure 1.2 Skeletal muscle development timeline. At E8.5, MuSCs expressing Pax3 and Pax7 from dermomyotome delaminate, migrate and begin to express MRFs, forming the primary myoblasts. Once in the myotome, these myoblasts differentiate into myocytes. At E11.5, primary myogenesis initiates when myocytes begin to fuse with each other and/or with the primary myoblasts to form primary myotubes. Secondary myogenesis starts at E14.5, in which proliferative MuSCs differentiate into secondary myoblasts and fuse with the primary myotubes. Continuous addition of new myotubes and fusion with myoblasts leads to skeletal muscle growth. In post-natal development, myotubes mature into myofibers and retain niches of Pax7-positive satellite stem cells that allow muscle growth and regeneration.

The Laminin composition of the BM varies according to the myogenesis stage. During primary myogenesis, laminin-containing BM are not detected around primary myotubes. At E14.5, when secondary myogenesis begins, laminins 211, 411 and 511 start to assemble around the myofibers and continue to grow. At E16.5, it was reported that Pax7-positive MuSCs begin to enter their niche under the myofiber BM and at E17.5 most of them are already located underneath the myofiber BM[19]. At E15.5, there is an increased deposition of laminins near the Pax7-positive MuSCs, which demonstrates the importance of laminins to support this crucial pool cells[19]. The MuSC pool is able to replenish itself or to differentiate into myoblasts, which is fundamental for myotube formation and muscle development. In adults, this niche constitutes a pool of quiescent precursors, located between the BM and the sarcolemma, that have an important role as they are able to divide and differentiate in response to growth factors for muscle growth or injury to replace the damaged muscle cells[38].

1.3.1 Myogenesis in *Lama2*-deficiency context

As previously mentioned, the host laboratory established that the onset of LAMA2-CMD in the dyW model for this disease, occurs during fetal development, between E17.5 and E18.5[19]. This study revealed that, between these fetal stages, laminin-211 deficiency leads to a significant reduction in the number of Pax7-positive and Myogenin-positive cells in dyW mice and a reduction in muscle growth, probably due to a reduction of MuSCs and a faulty muscle differentiation program in these mice. Moreover, as there is a reduction in the number of cells expressing Pax7 and Myogenin, later in adults, *Lama2* deficient mice reveal problems to regenerate injured muscles[8,19].

So far, these data suggest that the absence of *Lama2* impacts the capacity to promote MuSCs self-renewal and may prevent myoblast differentiation. As mentioned before, in normal conditions, the pool of Pax7-positive MuSCs is amplified by symmetrical divisions, giving rise to two identical Pax7-positive stem cells. The myofiber BM structure is crucial to maintain the self-renewals of the MuSCs pool, as a correctly assembled matrix creates the proper environment that favors symmetrical divisions, and loss of contact with BM may induce cell commitment (contact with BM maintains uncommitted state)[2,19]. Balanced asymmetric divisions also occur and originate one Pax7-positive cell and a committed cell that will later differentiate and fuse with a muscle fiber, increasing its size[36]. These asymmetric divisions are maintained after birth by the satellite stem cells. In the absence of laminin-211, Nunes et al. postulated that, due to a defective basement membrane during fetal development,

asymmetric divisions are promoted at the expense of symmetric divisions, leading to an extreme reduction of the Pax7-positive stem cell pool and an impairment in self-renewal. A possible explanation lies in myostatin deregulation and the overactivation of Janus kinase signal transducer and activator of transcription proteins (JAK-STAT) pathway[19], which can be mediated by an increase in the phosphorylation of the transcription factor STAT3 (pSTAT3) at Tyr705 in the dyW mice compared to wt mice. JAK-STAT signaling is involved in several cell fate pathways, including proliferation, differentiation, inflammation and immune system regulation and apoptosis[39] and therefore its overexpression may explain the decrease in the number of MuSCs and reduction in myofiber size.

1.4 Cell cycle regulation and survival in skeletal muscle in health and disease

In the absence of *Lama2*, the BM-cell membrane link mediated by α7β1 integrin is lost and the expression of this integrin is reduced[40]. This transmembrane integrin receptor is essential for the molecular connection between the BM and the myofibers and interferes in several processes. For example, α7β1 integrin regulates JAK-STAT3 pathway and its thought to attenuate STAT3 activation. So, when this integrin is absent, there is an increase in asymmetric divisions and precocious cell commitment[19]. The crosstalk between the BM and myofibers mediated by this integrin is also implicated in other processes like proliferation of MuSC/myoblast, differentiation and apoptosis[41].

The mechanisms linked to cell fate regulation are fundamental to control tissue homeostasis in mammals and other multicellular organisms. Cell fate pathways include proliferation/quiescence, apoptosis, autophagy and senescence, all of which have been described to play a role in skeletal muscle development and maintenance.

Cell division is a highly regulated process that occurs in every living organism and is fundamental for cells to proliferate, passing on the genetic information to the daughter cells. Cell cycle can be divided into five phases: G0 (cells that remain quiescent and correspond to the non-proliferative cells), G1 (cell growth and protein synthesis, duplication of cytosolic components), S (DNA replication), G2 (cell growth and mitosis preparation) and M-phase (mitosis and cytokinesis). This is regulated by several mechanisms that ensure genome integrity, cell division and survival, including checkpoints in different phases of cell cycle that allow, for example, DNA repair or that can induce programmed cell death if the damage cannot be repaired. The progression in each cell cycle phase depends on the correct regulation of the previous phase, and is orchestrated by the cyclins, cyclin-dependent kinases (CDKs), CDK-activating kinases (CAKs) and CDK-inhibitors (CKIs), which are primarily regulated by phosphorylation and dephosphorylation[42,43].CDKs form complexes with cyclins and promote activation and progress of the cell cycle. This is countered by CKIs, which negatively regulate CDKs. There are several known CDKs, which act in different cell cycle phases: CDK4, CDK6 and CDK2 act in G1 phase, CDK2 in S phase and CDK1 in G2 and M phases. These CDKs can form complexes with one or more cyclins – cyclins A, B, C, D, E, F, G and H. There are two families of CKIs: INK4 family and Cip/Kip family. INK4 family includes p15 (*Cdkn2b*), p16 (*Cdkn2a*), p18 (*Cdkn2c*) and p19 (*Cdkn2d*) and they bind to CDK4 and CDK6, preventing cyclin D activity. As CDK-cyclin D complexes are fundamental for G1 phase entry, when CKIs bind to the CDK, which prevent CDK-cyclin D complex formation, G1 entry and progression is inhibited. The Cip/Kip family is composed by p21 (*Cdkn1a*), p27 (*Cdkn1b*), p57 (*Cdkn1c*) and inhibit several CDK-cyclin complexes from different phases (Cdk1/cyclin A, Cdk1/cyclin B, Cdk2/cyclin A, Cdk2/cyclin E). There are several cell cycle checkpoints, but the main ones include: G1/S transition in G1 phase, G2/M transition in G2 phase and metaphase/anaphase transition in mitosis (spindle checkpoint)[43].

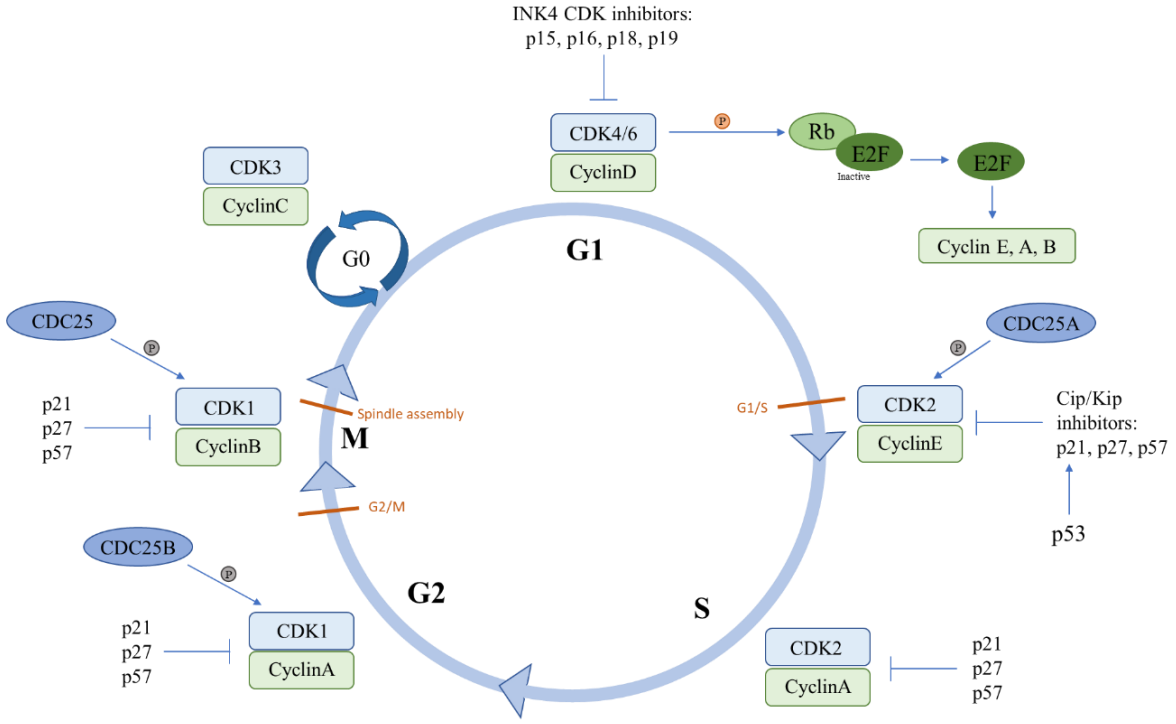

Figure 1.3 Cell cycle regulation through CDK/Cyclin complexes and CDK inhibitors. Cell cycle progression is orchestrated by several CDKs that are activated by different cyclins. Cells can enter a reversible quiescent state – G0 phase – which is regulated by CDK3/Cyclin C complex. CDK4/6/Cyclin D complex promotes cell cycle entry and progression. This complex phosphorylates retinoblastoma (Rb) protein, thus activating E2F transcription factors, inducing cyclin E, A and B expression. Cyclin E progressively activates CDK2 and this increases Rb phosphorylation, leading to S phase entry. Once in S phase, Cyclin E is replaced by Cyclin A, forming the CDK2/Cyclin A complex and progressing DNA replication. During later S phase, Cyclin A also forms a complex with CDK1, driving S-G2 transition. This complex remains until the end of G2 and is important for CDK1/Cyclin B formation and stabilization, resulting in mitosis entry. High concentrations of CDK1/Cyclin B complex induce M phase but when this complex is degraded, M phase is arrested and mitosis ends. Cdc25 phosphatases are involved in CDK activation by removing inhibitory phosphate residues and, when inhibited, act as checkpoint arrest. CDK-inhibitors (CKIs) belonging to either INK4 family or Cip/Kip family regulate CDK/Cyclin complexes. INK4 family CKIs (p15, p16, p18, p19) block CDK4/6/Cyclin D complex formation, thus preventing Rb phosphorylation and cell cycle progression. Cip/Kip CKIs (p21, p27, p57) inhibit the remaining CDK/Cyclin complexes.

1.4.1 Cell fate processes in skeletal muscle development and maintenance

In response to different endogenous and exogenous forms of stress and damage, cells may activate different pathways in order to cope with such challenges. For example, cells may enter a quiescence state characterized by reversible cell cycle arrest, in response to DNA-damage, aging or lack of nutrients. This state is also known as G0 phase, different from G1 phase, as these cells have the ability to re-enter cell proliferation when induced by different stimulus.

Despite playing a role against stress and damage, quiescence is also part of normal cell physiology. As previously mentioned, quiescence plays a critical role to maintain MuSCs stemness and self-renewal capacity in mature skeletal muscle[44,45]. Especially for adult satellite MuSCs, this is crucial to guarantee there is a pool of stem cells that can be activated and therefore proliferate and differentiate, in order to replace the damaged muscle fibers and promote tissue repair.

In contrast to quiescence, senescence corresponds to a state of irreversible cell cycle arrest, in which cells undergo morphological and functional changes, including cell enlargement, increased granularity, flattening, inhibition of telomerase activity and resistance to apoptosis, by expressing anti-apoptotic factors[46,47]. Cells undergo senescence as a response to prolonged stress, to avoid accumulation of damaged cells[48]. Some factors that induce this process include telomere shortening, DNA damage, oncogene activation and tissue damage. As a result, p53/p21, p53/p16 or p16/RB activation is promoted, leading to a permanent cell cycle arrest. Consequently, high levels of p21 and p16 are usually found in

senescent cells. A hallmark of senescent cells is the senescence-associated secretory phenotype (SASP), characterized by the secretion of several factors, namely interleukins, inflammatory cytokines, and growth factors, which act not only in the cells that express these factors, but also in surrounding cells (paracrine effect). This induces senescence and inflammation. In addition to the role of senescence as a response mechanism to prolonged damage, cell senescence also occurs as part of normal development[49]. During embryonic development, SASP factors secreted by senescent cells, recruit immune cells that remodel tissue by senescent cell clearance, fundamental for tissue growth and patterning[49,50]. Regarding adult MuSCs, senescent fibro/adipogenic progenitors (FAPs) recruit immune cells, which promotes MuSC activation and differentiation. Expression of SASP factors is then decreased when FAPs are eliminated by immune cells. Thus, a transient increase of senescence factors supports muscle regeneration[49].

In pathological context, impaired clearance of senescent cells promotes chronic accumulation of these cells, leading to a prolonged expression of SASP factors and consequently to chronic inflammation and fibrosis[49]. In line with this, MuSC senescence increases due to the production of SASP factors during the chronic inflammation process, thus leading to MuSC exhaustion and muscle regeneration impairment and progressive degeneration. As chronical senescent FAPS are anti-apoptotic, the accumulation of this factors results in muscle fibrosis[49].

Another cellular mechanism that impacts muscle homeostasis and disease is autophagy. This process is an intracellular quality control mechanism that removes damaged cell components, like organelles, lipids and proteins, through degradation via lysosomes[44,51,52]. This process is led by Autophagy-related (ATG) proteins, which are responsible for orchestrating the formation of double-membraned vesicles, called autophagosomes, which transport and deliver their content to be degraded in the lysosome. Basal autophagy maintains cellular homeostasis but in cases of nutrient deprivation or high energy demands, this process is crucial to provide nutrients and energy needed for cell survival by recycling intercellular components. Skeletal muscle imposes a high demand of energy, especially during physical activity. Bioenergetic control involves the degradation of mitochondria – mitophagy – important for cell metabolism and ROS regulation[44].

Autophagy and mitophagy were described to act in stem cell regulation, thus impacting on embryonic and postnatal development and repair during adult life. Autophagy is also responsible for senescence control in muscle, more specifically it is able to maintain stemness of the MuSC by preventing quiescence to senescence conversion[53]. In satellite MuSCs, autophagy also provides the energy needed during myogenic differentiation and the metabolic adaptations for cells to leave quiescence state and begin to proliferate. As an essential process to maintain skeletal muscle homeostasis, either deficient or excessive autophagy induce modifications including mitochondrial dysfunction, endoplasmic reticulum stress, cell damage and death, which can lead to several muscular dystrophies, evidenced by muscle atrophy and weakness[54].

Apoptosis is another cellular mechanism, which impacts on muscle homeostasis. It corresponds to a form of programmed cell death, activated by different types of stress and damage, such as hypoxia, lack of nutrients, DNA or other cell component damage, cytokines, oncogenes or viral infections[55]. Cells receive different signals that induce cell cycle arrest and, ultimately, when the damage is irreparable, cells either enter senescence or apoptosis[56,57]. When DNA damage is chronic, senescence is promoted while apoptosis is induced under acute damage.

Even though apoptosis has been first identified as an ultimate response to damage, it also plays essential roles in embryonic development. An example includes the need to maintain cellular homeostasis and control cell damage, proliferation and growth, either by expressing proapoptotic (e.g., Bax, Puma) or antiapoptotic (e.g., Bcl2) genes[56,58]. Also, it is required for tissue shaping during development by clearance of cells no longer needed, including during muscle patterning[59,60,61].

1.4.2 Role of p53 in skeletal muscle health and disease

Regulation of cell proliferation and survival can be orchestrated by different proteins, one of these factors being the tumor suppressor p53. p53 is a transcription factor that, when activated, can induce the transcription of multiple genes that regulate different biological functions, such as regulation of cell cycle, senescence, apoptosis, autophagy, enhanced DNA repair and differentiation and therefore is not surprising that is referred to as a "guardian of the genome". The choice of pathway to be induced strongly relies on p53 activation levels and co-activation of other proteins. For example, the decision between cell cycle arrest, quiescence and senescence, is closely associated with p53 and the mammalian target of rapamycin (mTOR) pathway activation. High induction of p53 inhibits mTOR and cells enter quiescence. Moderate p53 response is not enough to inhibit mTOR, inducing senescence [62]. Nuclear p53 is also thought to induce autophagy by promoting ATG gene expression and autophagy suppresses p53, whereas cytoplasmatic p53 is involved in autophagy inhibition[63].

One of the main apoptosis pathways is also mediated by p53. In this case, p53 induces cell cycle arrest through p21. Depending on the damage caused, p53 can induce apoptosis by activating Bcl-2-associated X protein (Bax), which links to the mitochondrial membrane, inducing mitochondrial depolarization and cytochrome c release. Cytochrome c leads to caspase cleavage and activation, being the caspases proteases enzymes that induce cell death[64].

p53 plays a central role in the response to multiple types of stress and damage, but it is also critical during normal development[65].

In the myogenesis context, regulation of p21 mediated by p53, induces cell cycle arrest of myoblasts during myogenesis, allowing them to stop proliferating and start differentiating to form myofibers. This shows the importance of cell cycle regulation for proper myogenesis (e.g., as mentioned before, MuSCs must exit proliferation to initiate differentiation via cell cycle arrest mediated by p53 and p21). *In vitro*, p53 was also demonstrated to have an important role in myogenesis. Hypothetically, in response to injury, quiescent satellite MuSC become activated and re-enter cell cycle (G1 phase). From the cell cycle results two daughter myoblast cells that can either continue dividing (re-enter cell cycle) or exit cell cycle. Cell cycle exit is induced by a transient p53 increase. After cell exit, the differentiation program is activated if cells return to basal expression levels of p53. Contrarily, an increased and prolonged p53 expression inhibits differentiation and the cell becomes quiescent, thus promoting asymmetrical division and self-renewal, and migration into their satellite cell niche[45].

1.4.3 Cell fate alterations in *Lama2* deficient context

Little is known about cell fate mechanisms during embryonic and fetal myogenic development in a laminin α2 deficiency context. Several signaling pathways are involved in myogenic differentiation, being JAK-STAT cascade pathway, activated by a variety of receptors (interferons (IFN) and interleukins (IL)) that cause different myogenic differentiation responses[66]. JAK1 is mainly involved in cell proliferation and JAK2 and JAK3 act in differentiation. Together with JAK1, STAT1 or STAT3 can act by inhibiting myoblast differentiation in C2C12 cells[66]. JAK2-STAT3 signaling pathway was shown to promote myogenic differentiation through MyoD induction. On the contrary, JAK3-STAT3 negatively regulates differentiation. Therefore, JAK-STAT signaling is crucial to maintain tissue homeostasis and is implicated in various mechanisms. Using the dyW mouse model of LAMA2-CMD, Nunes et al showed that JAK-STAT3 target gene *Pim1* is significantly increased in muscle tissue in the absence of *Lama2* at E17.5[19]. Pim1 is a factor associated with numerous cell fate processes, including cell survival, cell cycle, senescence and cell growth, suggesting alterations in one of these cell fate pathways. Also, activated STAT3 is significantly increased in postnatal 2 (PN2) stage muscles and phosphorylation levels are even higher in 3-week-old mice.

Previous studies showed that JAK-STAT pathway overactivation impairs muscle repair and promote aging[67,68]. This overactivation of STAT3 signaling leads to an increase in MyoD expression,

which in turn activates p21 and induces precocious cell cycle exit, resulting in decreased number of differentiated cells[19]. In addition, Nunes et al showed that an increased phosphorylation of STAT3 in PN2 muscles does not occur due to augmented inflammation and fibrotic tissue accumulation. Rather they hypothesized that JAK-STAT overexpression could inhibit MuSCs symmetric divisions, contributing to early myogenic commitment and reduction of MuSC pool.

Damage caused by the absence of laminin α2 chain of laminin-211, can lead to the overactivation of several cell fate markers such as p21 and Bax, which promote cell cycle arrest and apoptosis, respectively, both regulated by p53. In addition, it was found that p53 mediates aberrant caspase activation in the context of laminin-α2-deficiency, leading to increased apoptosis during the progression of the disease[69]. The results demonstrated the possibility that p53 inhibition could attenuate the characteristic phenotype of LAMA2-CMD. *In vitro*, p53 signaling was also reported as a regulator of the balance between differentiation and self-renewal of MuSCs after muscle injury[45]. Thus, a deregulation of p53 and the pathways associated with it can lead to alterations in terms of the maintenance of quiescence in MuSCs and myoblast differentiation.

Ubiquitin-proteasome pathway, in which faulty and damaged proteins are degraded, was also shown to be increased in the dy^{3k}/dy^{3k} mouse model[70]. Autophagy gene expression were upregulated in LAMA2-CMD and autophagy inhibition resulted in phenotype improvement[70]. Probably linked to this, an increase in metabolism was verified, possibly to support the energy demands needed and compensate for mitochondrial dysfunction. This bioenergetic deregulation disturbs cell balance and leads to increased myoblast apoptosis[71].

1.5 Aims of the project

Increased STAT3 phosphorylation has been shown to be a primary event in LAMA2-CMD and it is well established that this pathway triggers important signaling cascades that are involved in cell cycle regulation and cell survival. However, it is not clear which pathway or pathways are altered at the onset of LAMA2-CMD. A better understanding of what fails in the context of LAMA2-CMD is imperative for the development of new therapies. This project aimed at analyzing which cell fate mechanisms are altered during the onset of this disease and whether they can be countered by deletion of *p53*. To address this, the following task were undertaken:

- → Analyze pathways linked to cell cycle regulation and survival that might be altered in the absence of *Lama2 in vivo*, in order to have a better understanding of the mechanisms that trigger the appearance of this condition and can open new paths for the treatment
- → Establish and test *in vitro* myoblast cell line models to study laminin α2 deficiency.
- → Test if *p53* deletion in a *Lama2*-deficient context improves the LAMA2-CMD phenotype *in vitro*.

Chapter 2 Methodology and Materials

2.1 Mice and fetus collection

The project used an established line of genetically modified (dyW) mice, which is the most studied and frequently used mouse model for LAMA2-MD pathogenesis[8] (www.curecmd.org/resources-for-scientists). Colony breedings (Ethics Protocol A005-2019) were kept at Instituto Gulbenkian Ciência in a specific pathogen free animal facility.

E17.5 and E18.5 homozygous dyW and WT fetuses were obtained by crossing heterozygous dyW C57BL/6 mice. Confirmation of pregnancy was made by the presence of plugs on E0.5 and by weighing the females before they were sacrificed, which was performed by licensed team members (DL113/2013). Pregnant females were anesthetized with isoflurane, sacrificed by cervical dislocation

and the uterine horns were removed and placed in ice-chilled PBS. Fetuses were removed from the uterine horns, maintained in ice-chilled PBS, decapitated and the tails were cut for genotyping.

Deep back muscles were isolated and used in the different experimental setups or kept at -80 °C for long-term preservation.

Our research was conducted in agreement with the European Directive 2010/63/EU and Portuguese legislation (Decreto-Lei 113/2013, Decreto-Lei 1/2019). The researchers that handle the mice are experienced and are licensed form the national authority (DGAV; DL113/2013).

2.1.1 Genotyping

For genotyping, an ear punch used to identify the animals was placed into an Eppendorf tube. Then, 25 mM NaOH / 0,2 mM EDTA was added to the tube and placed in thermocycler at 95 °C for 30 min, followed by cooling the tubes to 4 °C. Next, 40 mM Tris HCl pH 5,5 was added to the mixture in a 1:1 ratio and centrifuged at 4000 rpm for 3 min. For PCR, 1 µL of undiluted mixture was used per PCR tube. All PCR reactions were performed using Xpert Fast Hotstart DNA Polymerase (GRISP) according to the manufacturer's instructions. To perform genotyping of dyW, a single mix was prepared with primer 1, primer 2 and primer 3. For p53 genotyping, two different mixes were prepared separately: wt mixture prepared with Dop53 Rev primer and Dop53 WT primer; Neo mixture with Dop53 Rev primer and Dop53 Neo primer. All primer sequences used are listed in Annexes Table S.1. PCR was performed according to the protocol in Annexes Table S.2.

2.2 Real Time-qPCR

2.2.1 RNA Extraction

Epaxial muscles were isolated from the fetuses and stored at -80 °C. Samples were homogenized in 500 µL of TRIzol™ Reagent (Invitrogen™) using a tissue homogenizer (Retsch MM400 Tissue Lyser). For C2C12 cells, samples were lysed in 500 µL of TRIzol™ Reagent Then, the tubes with the samples were incubated for 5 min to allow complete dissociation of the nucleoprotein complexes and 100 µL of chloroform was added. All tubes were incubated for 2–3 min and centrifuged for 15 min at 12,000 g at 4°C. The mixture separated into a lower red phenol-chloroform, an interphase, and a colorless upper aqueous phase. The aqueous phase containing the RNA was transferred to a new tube. For the epaxial muscles, interphase and organic phase was saved to proceed with protein extraction (See *3 a) Protein extraction* method below). Next, 250 µL of isopropanol were added to the aqueous phase to precipitate de RNA and samples were incubated for 10 min and then centrifuged for 10 min at 12,000 g at 4°C. The supernatant was discarded. The pellet was washed twice in 500 µL of 75% ethanol and then centrifuged for 5 min at 7500 g at 4°C. All ethanol was removed, and the pellet was air dried. The pellet was resuspended in 20–50 µL of RNase-free water, placed on ice and incubated at 55°C for 10 min. RNA concentrations were determined in a Nanodrop and the quality of the RNA was assessed by the analysis of 260/280 and 260/230 ratios.

2.2.2 cDNA and RT-qPCR

Complementary DNA (cDNA) was synthesized from a single-stranded RNA template (obtained in the previous section a) RNA extraction), in a reaction catalyzed by reverse transcriptase enzyme using the Xpert cDNA Synthesis Kit. Briefly, the following components were added to a RNase-free microtube: 1µL dNTP mix, 1µL random hexaprimer, RNase free water and 1µg RNA obtained after RNA extraction. The mixture was placed in a thermocycler: 65ºC for 5 min, then placed on ice for 2 min. After that, 4µL 5x Reaction Buffer, RNase inhibitor (40U/µl) and Xpert RTase (200U/µl) were added and the mixture was placed in a thermocycler at 25°C for 10 min, 50°C for 50 min and 85°C for 5 min. The obtained cDNA was stored at -20ºC to be used as a template for Real-Time qPCR.

For the Real-Time qPCR (RT-qPCR) reaction, SsoAdvanced Universal SYBR® Green Supermix or iTaq™ Universal SYBR® Green Supermix (Bio-Rad) were used as a high-performance real-time PCR supermix. First, all reaction components were mixed thoroughly and stored on ice protected from light. Reaction mix for PCR reaction was prepared, without the DNA template: Universal SYBR Green Supermix (2x), forward and reverse primers (specific for each gene analyzed) and nuclease-free H_2O. All primer sequences used are listed in Annexes Table S.3. Then, 1 µL of cDNA was added to each well of a 96-well plate containing the reaction mix, the plate was sealed with an optically transparent film and centrifuged to remove all air bubbles in the wells and to ensure that the mixture stayed at the bottom of the well. Finally, the plate was placed in the CFX96™ Real-Time PCR Detection System (Bio-Rad) with the protocol Annexes Table S.4. After the PCR run, data analysis was performed by analyzing the threshold cycle (Ct) values and comparing the Ct value of the gene of interest (GOI) and the one selected as housekeeping gene, according to the following equations:

$$\Delta \mathrm{Ct} = \mathrm{Ct}_{\mathrm{Housekeeping}} - \mathrm{Ct}_{\mathrm{GOI}} \quad (2.1)$$

$$\text{Fold difference to housekeeping} = 2^{\Delta \mathrm{Ct}} \quad (2.2)$$

For all the genes in all PCR reaction the quality was assessed by the analysis of the melting curves.

2.3 Western Blot

2.3.1 Protein extraction

- Tissue samples

In order to comply with the 3R policy of animal welfare, the same fetal muscle sample was used for both RNA and protein extraction. At the RNA extraction step (*2.2 Real Time-qPCR a)RNA Extraction*), while the colorless aqueous phase was collected for RNA extraction, the interphase and organic phase were kept in the microcentrifuge tubes to proceed with protein extraction. The DNA was in the interphase and the proteins in the lower red phenol-chloroform phase. First, as much as possible of the remaining aqueous phase left in the tube was removed to prevent RNA from being collected with the DNA and proteins (critical for the quality of the isolated proteins). After that, 150 µL of 100% ethanol was added to precipitate the DNA, followed by mixing by inversion of the tube several times. The mixture was incubated for 2-3 min and centrifuged for 5 min at 2000 xg at 4ºC, thus obtaining the pellet containing the DNA. The phenol-ethanol supernatant was transferred to a new tube and this was used to proceed with protein isolation. Then, 750 µL of isopropanol were added, and the sample was incubated for 10 min, and centrifuged for 10 min at 12,000 × g at 4°C to obtain the protein pellet. The supernatant was discarded with a micropipette. Next, the pellet was resuspended in 1 mL of wash solution (0.3 M guanidine hydrochloride in 95% ethanol) and incubated for 20 min. The tubes were centrifuged for 5 min at 7500 × g at 4°C and the supernatant was discarded. This washing procedure was repeated twice. Next, 2 mL of 100% ethanol was added and the samples were mixed by vortexing and then incubated for 20 min at room temperature (RT). The tubes were again centrifuged for 5 min at 7500 × g at 4°C and the supernatant was discarded. The protein pellet was air dried for 5-10 min. To solubilize the proteins, the pellet was resuspended in 200 µL of 2x SDS-PAGE sample buffer (20 % Glycerol, 4 % SDS 100 mM, Tris pH 6.8, 0.2 % Bromophenol blue and 100 mM DTT) by pipetting up and down. The samples were incubated at 50°C for 10 min in a thermomixer and centrifuged for 10 min at 10,000 × g at 4°C. Finally, the supernatant resulting from the last centrifugation was transferred to new tubes and protein quantification was performed using Nanodrop, measuring the absorbance at 280 nm. The samples were stored at -20°C until further use.

– C2C12 samples

Cells were pelleted and resuspended in 100 µL of 2x SDS-PAGE sample buffer. Cell lysates were then incubated with benzonase at RT for 10 min, to degrade DNA and RNA. Cells were heated at 50°C for 10 min and centrifugation at maximum speed for 5 min. The supernatant was transferred to a new microcentrifuge tube and Nanodrop was used to determine protein quantification measuring the absorbance at 280 nm.

2.3.2 Western Blot

Since the proteins under analysis range from 15-124 KDa, a 12% polyacrylamide gel was used to separate protein samples. After loading the samples in the gel (150µg – cells; 15µg – muscle), these were electrophoresed in 1x Running Buffer (3.02 g Tris base, 14.42 g Glycine, 1 g SDS, up to 1 L distilled water) during 1 hour at 150V, using the Mini-PROTEAN® Tetra electrophoresis system (Bio-Rad). The gel was then mounted in a transfer cassette with the polyvinylidene fluoride (PVDF) membrane, previously activated with methanol. Proteins were then transferred in chilled Transfer Buffer (5.82 g Tris, 2.93 g glycine, up to 1 L distilled water) on a bed of ice for 45 min at 100V, Mini Trans-Blot® Cell (Bio-Rad). After transfer, the gel was stained for 1 hour with GelCode™ Blue Safe Protein Stain (ThermoFisher Scientific) to confirm quality of protein extracts and to verify the loading of the gel. The membranes were blocked using 5% powdered milk in TBST (20 mM Tris, 150 mM NaCl, 0.1 % Tween20 and distilled water, pH 7.4-7.6) for 1 hour with agitation. Membranes were rinsed in TBST 3 times and incubated with the primary antibody, diluted in 2% bovine serum albumin (BSA) in TBST and 0.02% Sodium Azide overnight at 4°C with agitation (Antibodies and dilutions used are listed in Annexes Table S.5). The following day, membranes were washed in TBST and incubated with secondary antibody coupled with horse radish peroxidase (HRP) diluted in 5% powdered milk in TBST for 1 hour at RT. Membranes were washed 3 times, for 10 min each, in TBST and chemiluminescence was detected using Supersignal™ West Pico Chemiluminescent Substrate HRP (ThermoFisher Scientific). Images were acquired using the Amersham Imager 680 RGB (GE Healthcare).

2.4 Establishment of tools for CRISPR/Cas9 mediated deletion

CRISPR/Cas9 can be used to generate knock-out (ko) cells by co-expressing a guide RNA (gRNA) specific to the gene to be targeted and the endonuclease Cas9[72]. The gRNA has a 20bp target sequence complementary to the target gene and lies next to the protospacer adjacent motif (PAM). The PAM sequence is crucial for Cas9 binding and activation. In order to obtain gRNA targeting *Lama2* and *p53* two approaches were used. In the first approach gRNA were designed and cloned in to the pX330 vector. pX330 is a vector that allows to clone the gRNA of interest and is simultaneously able to express the Cas9 endonuclease. For this approach one gRNA targeting *p53* was cloned into pX330 and used for CRIPR/Cas9 mediated deletion (see protocol details below). In the other strategy, validated gRNA were directly acquired from VectorBuilder, in the format of a mammalian expressing vector, containing Cas9 and puromycin resistance gene (pRP[CRISPR]-Puro-hCas9-U6). Two gRNA targeting *Lama2* together with two targeting *p53* were used to delete each gene. This strategy aims at ensuring successful knockout of these genes. The gRNA sequences are listed in Annexes Table S.6.

2.4.1 Preparation of chemically competent *E. coli*

Pre-culture was made from *Escherichia coli* growing on Lysogeny Broth (LB) agar plate. For that, a single colony was grown overnight at 37°C in 10 mL of LB. Next, 150 mL pre-heated LB was inoculated with this pre-culture in a 1/100 ratio and incubated with shaking at 37 °C for about 2-3 hours (until the culture reached OD600 ~ 0.4). Then, 45 mL of culture were distributed into two 50 mL Falcon tubes and placed on ice for 10 min. From this point, the tubes were always kept on ice. Tubes were centrifuged at 2700 g for 10 min at 4°C. The supernatant was quickly decanted and the tubes inverted,

allowing to remove all the remaining liquid. The pellet was gently resuspended with 13,5 mL of 80 mM $MgCl_2.6H_2O$ / 20 mM $CaCl_2.2H_2O$ solution for each 45 mL of starting medium. Tubes were again centrifuged at 2700 g for 10 min at 4°C and the supernatant was completely removed. The pellet was gently resuspended in 1,8 mL of 100 mM $CaCl_2$ / 15% glycerol solution, for 45 mL of initial culture, and distributed in 150 µL aliquots and frozen at -80 °C.

2.4.2 CRISPR/Cas9 for gene deletions in cell lines using PX330

To clone the p53 gRNA3 into pX330, the plasmid was digested with BbsI for 1h at 37ºC, which generated sticky ends (single stranded DNA). Digested pX330 was gel purified and eluted in ddH2O and then the DNA concentration was analyzed. The gRNA was designed as two individual oligonucleotides (sense and anti-sense sequences), which were then annealed using 1X T4 ligation buffer and the mixture was placed in a thermocycler: 37°C for 30 min, 95°C for 5 min and then ramp down to 25°C at 5°C/min. BbsI digested pX330 was mixed with 1:100 dilution of annealed oligo duplex, T4 ligase buffer, T4 ligase enzyme and ddH_2O. Ligation reaction was set up at RT for 30 min. After 30 min, BbsI was added to the mixture and incubated for additional 15 min.

2.4.3 Bacterial transformation

For this procedure, three different plasmids were used: pX330, pEGFP and pSuperior Retro Puro. pEGFP was used as a control to optimize the transfection conditions. pSuperior Retro Puro plasmid served to test puromycin resistance, in order to establish the protocol to select the cells that were successfully transfected.

For bacterial transformation, first, a tube of competent *E. coli* cells was thawed on ice for 10 min and then 1-5 µl containing 1 pg-100 ng of plasmid DNA was added to the cell mixture and the tube carefully flicked 4-5 times to mix cells and DNA. The mixture was placed on ice for 30 min. Then, a heat shock was applied at 42 °C for exactly 30 sec. After the heat shock, the mixture was again placed on ice for 5 min. LB was added and transformed bacteria were then placed at 37°C for 60 min with vigorous shake (250 rpm). The bacteria were incubated under these conditions to recover from chemical transformation and allow time to express the antibiotic resistance gene present in plasmids. Before plating, the mixture was centrifuged, most of the supernatant removed and the pellet resuspended very well (in the remaining supernatant). Finally, the resulting mixture was plated on LB agar with ampicillin or kanamycin selection and incubated overnight at 37°C. The next day, an ampicillin (pX330 and pSuperior Retro Puro) or kanamycin (pEGFP) resistant colony was collected for each plasmid and allowed to grow in a liquid medium. Colonies were screened by colony PCR using PX330_seq fwd: AGTACAAAATACGTGACGTAG and p53_gRNA3_rev: AAACATGGTGATGGTAAGCCCTCAC. The selected colonies were then grown in LB and part of the culture obtained was used to make a bacterial stock using 50% glycerol and another part used to purify the plasmid for transfection of C2C12 myoblast cell line. The commercial plasmids from VectorBuilder were provided as frozen bacterial stocks and plasmids were extracted as described above.

2.5 *In vitro* procedures

2.5.1 Cell culture

C2C12 is an immortalized myoblast cell line derived from mouse skeletal muscle satellite cells often used as model to study the myogenic process[73]. When C2C12 cells are confluent, they begin to differentiate, giving rise to elongated myocytes that afterwards fuse with each other to form the myotubes. C2C12 cells were grown in Dulbecco's Modified Eagle's Medium (DMEM), supplemented with 10% fetal bovine serum (FBS) and 1% antibiotics (complete medium). Cells were kept in culture at 37ºC, 5% CO_2 and constant humidity and were passaged frequently, using trypsin-EDTA, when 70% confluency was reached, or the medium was removed and replaced every 2-3 days.

2.5.2 Optimization and transfection procedure

Transfection of C2C12 cells was optimized using Lipofectamine 3000 transfection reagent and the pEGFP plasmid. For that, cells were plated on a 6-well plate for transfection (3 x 10^5 cells per well to allow for 70-90% confluency on the day of transfection) and two different conditions were tested – condition A and condition B. In condition A, cells were allowed to grow in complete media for 24h. The next day, the transfection was done by replacing complete media with the transfection mix and without trypsinizing the cells (forward transfection). In condition B, cells were grown in DMEM supplemented with 10% FBS without antibiotics for 24h. After that, trypsin was added until cells where rounded, but not detached. All trypsin was removed carefully, and cells were resuspended and plated in the transfection mix (reverse transfection).

For transfection, the mix was prepared according to the manufacturer's instructions (Thermo Scientific). Briefly, Lipofectamine 3000 reagent (5,5 µL) was diluted in optiMEM medium. In another tube, DNA mix was prepared by diluting 1µg of plasmid in optiMEM medium, then P3000 reagent was added and mixed well. The transfection reagent and DNA mixtures were combined in a 1:1 ratio and incubated for 15 min. The medium previously present in the plate was removed and the mix and DMEM medium without antibiotics was added to the cells.

2.5.3 Puromycin selection

Selection of transfected cells was optimized to determine the best concentration and time of incubation with puromycin. For that C2C12 cells where transfected using pSuperior Retro Puro, which contains a puromycin resistance cassette. Selection with puromycin was started 24h or 48h after the transfection, 10% FBS DMEM without antibiotics was replaced by complete medium and puromycin (1, 2 or 3 µg/mL) was added to each of the wells on the plate. Cells were incubated for 48h and cell death was analyzed.

2.5.4 Establishment of CRISPR/Cas9 cell lines

The final transfection protocol executed was the one from condition B, mentioned in section *2.5 In vitro procedure b) optimization and transfection procedure*. The DNA mix used included PX330 plasmids that had puromycin resistance gene and the respective gRNA targeting *Lama2* or *p53*.

After puromycin selection, part of the cells was harvested and RNA was extracted from each pool of cells obtained (*Lama2* ko, *p53* ko and *Lama2/p53* ko), and RT-qPCR was performed as described previously. RT-qPCR was used to evaluate transfection efficiency by determining the reduction in the expression of the targeted genes comparing mutant and Wt C2C12 cell lines. Then, limiting dilution cloning was used to isolate single cell clones, more precisely the homozygous ko cells with the mutations in both alleles. First, cells were trypsinized and resuspended in complete DMEM media. Cells were then counted and diluted in order to obtain a density of 8 cells/mL in DMEM with 20% FBS and 1% antibiotics. Next 100 µL of this cell suspension was transferred into each well (0,8 cells/well) in a 96-well plate. This process was performed for the three knockout mutant groups (*Lama2* ko, *p53* ko and *Lama2/p53* ko) in duplicate. The cells were incubated at 37°C and scanned daily to identify wells with a single colony. The efficiency of the deletion of the gene of interest (*Lama2* and/or *p53*) was analyzed by RT-qPCR and the colonies with lowest levels of expression of the target genes were selected for further characterization.

2.6 Immunofluorescence

On the day before the experiment, C2C12 cells (Wt and selected clones) were plated in a 24-well plate. Coverslips were added to each well and then 50 000 cells, per well of each line, were plated. Cells were washed with 1x PBS and fixed for 10 min with 4% paraformaldehyde in PBS, at RT. After washing again with PBS, cells were permeabilized in 0,1% Triton-X100 in PBS for 5 min and washed twice with PBS. Then, cells were blocked with blocking solution (1% BSA, 1% goat serum, 0.05%

Triton-X100 in PBS) for 1h at RT and incubated with the primary antibody (Annexes Table S.5) diluted in blocking solution overnight at 4ºC. The following day, cells were washed twice with blocking solution and incubated with the secondary antibody (Annexes Table S.5) diluted in blocking solution for 1h at RT. Nuclei were stained with DAPI (4′,6-diamidino-2-phenylindole) for 30 sec. The cells were rinsed with water and the coverslips removed from the plate and left to dry for 30 min. Finally, samples were mounted using mounting media (50 mg/ml propyl gallate in PBS:glycerol, 9:1) Images were acquired using an Olympus BX60 fluorescence microscope.

2.7 Resazurin proliferation assay

To analyze the proliferation of the different C2C12 cells, a resazurin assay was performed. For that, on the day before the experiment, the cells were plated in a 96-well plate (5000 cells per well). The next day, cells were incubated in 120 µL 1x Resazurin solution in complete DMEM medium for 1h20min. This day corresponds to day 0. Fluorescence (excitation filter 531/40 nm; emission filter 595 nm) was measured using Victor 3V plate reader on day 0, 1, 2 and 5. The fluorescence levels were normalized using a control well containing 1x Resazurin solution in complete DMEM without cells.

2.8 Cell cycle analysis by Flow cytometry

The different C2C12 cell lines were collected from a T25 flask, placed in an Eppendorf tube and washed in 1x PBS. After washing and discarding the PBS, cells were resuspended in 300 µL of PBS and 700 µL of ice-cold absolute ethanol and fixed at -20°C for at least 24h. Immediately before starting the cell cycle analysis by flow cytometry, samples were centrifuged at max speed for 5 sec (to form a pellet) and the ethanol was discarded with a micropipette and replaced by PBS. Centrifugation and the PBS wash were repeated. The cell pellet was resuspended in 450 µL of PBS and 50 µL of 5 mg/mL RNase and incubated for 5 min at RT. Samples were centrifuged and resuspended in 500 µL of PBS plus 200 µL of 50 µg/mL Propidium iodide. Cell staining with propidium iodide, a fluorescent dye that intercalates into double-stranded nucleic acid, was used to analyze cell cycle distribution, based on the amount of DNA present in each cell. The analysis by flow cytometry was performed using the BD FACSCalibur™ Flow Cytometer (BD Biosciences) and the data obtained was processed and analyzed using Flowjo_v10.8 software or Mod Fit LT 5.0.

Chapter 3 Results

Impact of *Lama2-deficiency* in the expression of genes linked to cell fate regulation in skeletal muscle *in vivo*

Using the dyW mouse model of LAMA2-CMD, the onset of the disease was previously shown to occur between embryonic stages 17.5 and 18.5 (E17.5 and E18.5), where most significant alterations were observed, including reduction in the size of muscle fibers and lower expression of the myogenic factors Pax7 and Myogenin[19]. These alterations may be related to changes in the regulation of the cell cycle and cell survival. This was revealed by the higher phosphorylation levels of STAT3, a key transcription factor involved in multiple signaling pathways, as well as increased expression of the respective target gene *Pim1*[19] , known to regulate several cell cycle and survival pathways. In accordance, it has been shown that there is an increase in apoptosis and autophagy in post-natal *Lama2* deficient mice[69,70,74].

To investigate how *Lama2*-deficiency impacts on cell cycle regulation and survival, the expression of genes linked to proliferation/quiescence, apoptosis, senescence and autophagy pathways were analyzed by RT-qPCR. For that, epaxial muscles from wildtype (wt) and dyW mice at E17.5 and E18.5 were collected. The RNA was extracted and converted into cDNA, followed by the determination of mRNA expression levels by RT-qPCR (Figure 3.1).

Regarding the analysis of genes linked to quiescence and proliferation (Figure 3.1 A), the expression of *Cdkn1a* (encoding p21) from dyW fetal muscle at E17.5 was significantly increased compared to wt fetuses and at E18.5, the same tendency is maintained although statistical significance is not reached. *Cdkn1c* gene expression (encoding p57) was also significantly increased at E17.5, but the same was not observed at E18.5. As p21 and p57 act in the same cell cycle stage, both increased expressions may contribute to an overwhelmed increased cell cycle arrest. Also, *Pim1* expression was significantly upregulated in E17.5 dyW muscles, but this increased expression no longer occurs at E18.5. The expression of *Mki67*, which is a marker of cell proliferation, was found to be significantly downregulated in E18.5 dyW compared to wt mice, suggesting a reduction in cell proliferation in dyW muscles compared to wt. Analysis of mRNA expression of the pro-apoptotic *Bax* gene expression demonstrates a tendency to be decreased compared to wt mice. The anti-apoptotic *Bcl2* gene did not show significant differences (Figure 3.1 B). Autophagy was also analyzed, by looking at the expression of two genes linked to this process – *Atg7* and *Lamp2a* (Figure 3.1 C). Autophagy is an important mechanism that cells use to degrade and remove damaged or unnecessary cellular components but, when overactivated, can lead to cell degeneration[75]. Results show a significant upregulation of *Atg7* gene in E18.5 dyW mice and a similar tendency for *Lamp2a*. Finally, senescence, in which cells enter an irreversible arrest of the cell cycle, was another process addressed in this study. This process was analyzed through expression levels of two genes involved in the senescence pathway, *Il-6ra and Ccl7* (Figure 3.1 D). Analysis of both genes in E17.5 showed a tendency for increased *Il-6ra* gene expression in dyW fetal muscle in comparison to wt and this was even more evident for *Ccl7*, where the expression was significantly increased in E17.5 and in E18.5 dyW fetuses when comparing to wt controls. Overall, these data suggest alterations in genes involved in proliferation, senescence, and autophagy in the muscles of dyW fetuses compared to wt.

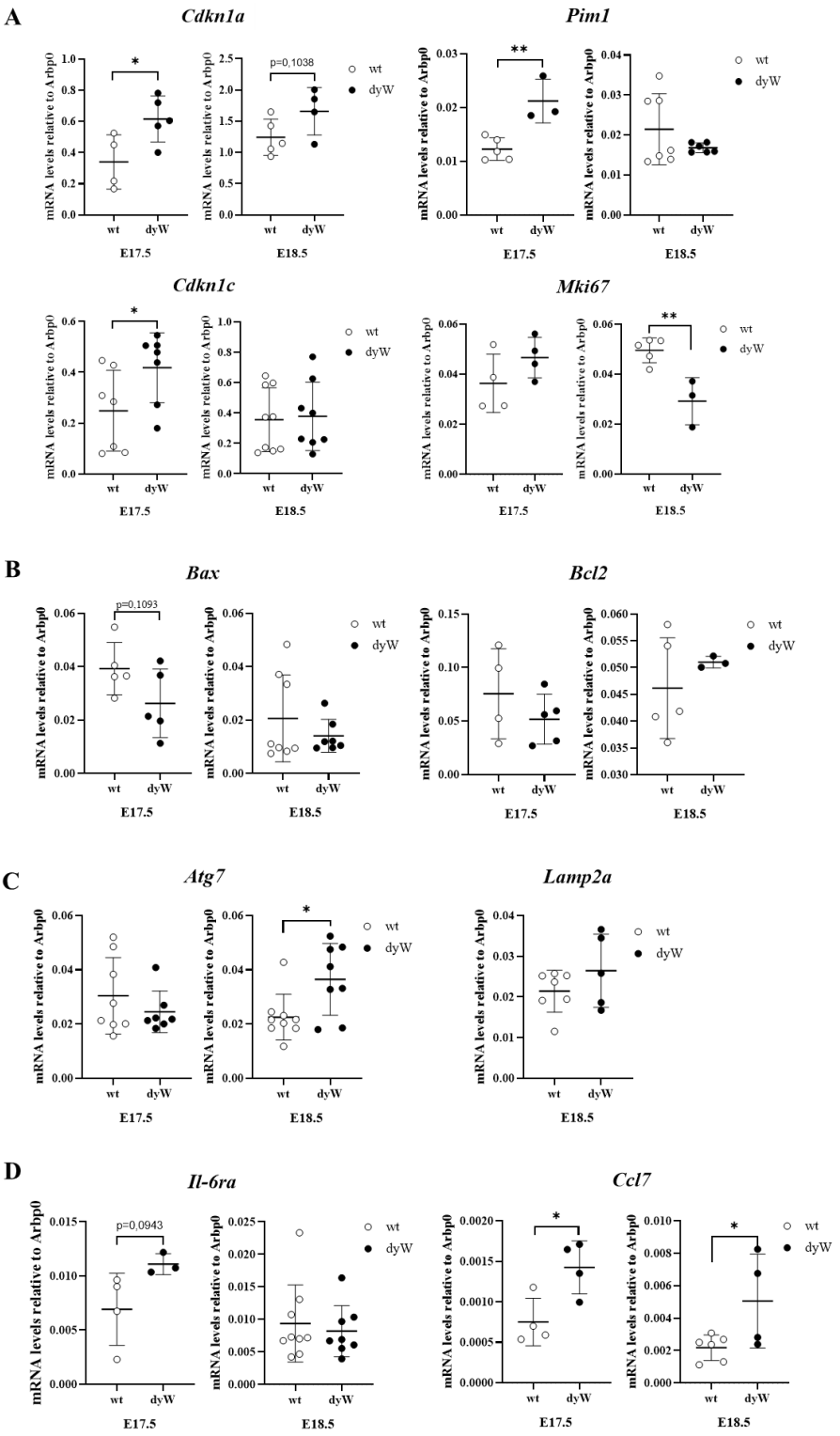

Figure 3.1 *Lama2*-deficiency impacts on the expression of genes involved in proliferation/quiescence, senescence and autophagy. Epaxial muscles were collected from wildtype (wt) and dyW-/- mice at E17.5 and E18.5 and RNA was extracted. Expression of cell fate genes linked to (A) Proliferation/quiescence – *Cdkn1a*, Pim1, *Cdkn1c* and *Mki67*, (B) Autophagy – *Atg7* and *Lamp2a*, (C) Apoptosis – *Bax* and *Bcl2*, and (D) Senescence – *IL-6ra* and *Ccl7*, was analyzed RT-qPCR and normalized using the housekeeping gene Arbp0. Statistical analysis was done using student's *t*-test. P-value: * p<0.05; ** p<0.01. n = 3-8 fetuses per genotype.

Impact of *Lama2-deficiency* on proteins linked to cell cycle and survival in skeletal muscle *in vivo*

JAK-STAT signaling pathway promotes *Pim1* expression, a gene involved in several cell fate pathways. The direct binding of pSTAT3 to the *Pim1* promotor upregulates *Pim1* gene expression. Results from the previous section showed an increased expression of *Pim1* at E17.5 (Fig. 3.1A). Increased activation of STAT3 is known to promote muscle atrophy in muscular dystrophies[76]. In addition, as mentioned before, JAK-STAT overactivation is also thought to favor asymmetric divisions[68], which specially impacts MuSC pool proliferation and formation during fetal myogenesis. STAT3 can be activated by phosphorylation, including phosphorilation of two residues – Tyr705 or Ser727 – depending on the ligand stimulus received. pSTAT3 Tyr705 promotes homodimerization of STAT3, which leads to nuclear translocation and DNA binding and pSTAT3 Ser727 promotes the translocation of STAT3 to the mitochondria, where it increases electron transport chain activity by interacting with the enzyme complexes that comprise the respiratory chain[77]. While total STAT3 is not altered in muscular dystrophy cases[19,76], previous work from the host laboratory using SureFire analysis suggests that there may be an increase in pSTAT3 (Tyr705) levels already in E17.5 dyW muscles, which is statistically significant at PN2[19].

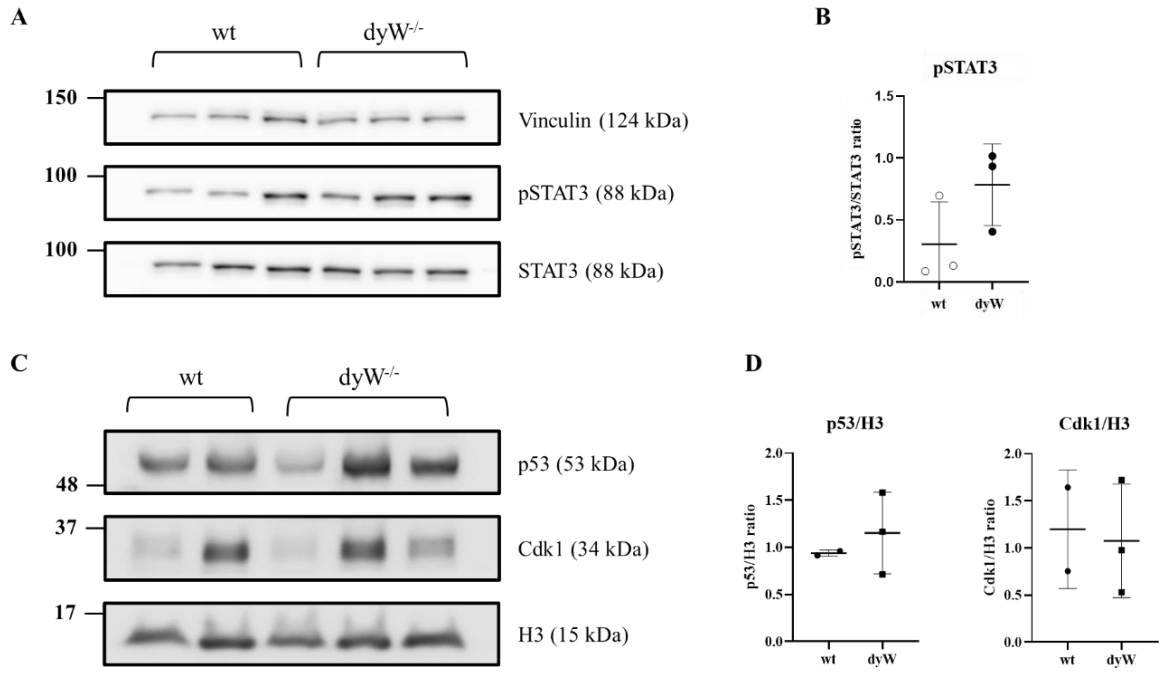

Figure 3.2 Expression of proteins linked to cell cycle regulation and cell fate is altered by the deletion of the *Lama2*. (A) Western blot analysis was performed using epaxial muscle collected from wildtype and dyW$^{-/-}$ mice at embryonic stage 17.5 (E17.5) to determine the protein expression levels of pSTAT3 (Tyr 705), STAT3. Vinculin was used as loading control. (B) Quantification of STAT3 by calculating pSTAT3/STAT3 ratio. (B) Western blot analysis was performed using epaxial muscle collected from wildtype and dyW$^{-/-}$ mice at E18.5 to determine the protein expression levels of p53 and Cdk1. Histone 3 (H3) was used as loading control. (D) Quantification of p53 and Cdk1 protein expression normalized using H3. n = 2-3 fetuses per genotype.

Consistent with previous work from the host laboratory, expression levels of pSTAT3 Tyr705, though not significant, tend to be increased in dyW compared to wt fetuses, at E17.5 (Figure 3.2 A, B). Preliminary data also showed a tendency for p53 to be increased in dyW mice (Figure 3.2 C, D), suggesting that the alterations concerning cell cycle regulation may be caused by this increased expression of this transcription factor. However, more samples are required to further confirm this altered expression. Cdk1 (*Cdc2*), cyclin dependent kinases needed for mitosis progression, showed no alterations between genotypes. This showed that there is no induced arrest of G2/M phase.

Lama2* and/or *p53* deletion by CRISPR-Cas9 in C2C12 cells *in vitro

One of the aims of this project was to establish an *in vitro* model to study LAMA2-CMD. For that, CRISPR/Cas9 technique was applied to obtain knockout C2C12 cell lines by transfecting plasmids containing puromycin resistance gene and a specific gRNA. The goal was to generate three different C2C12 cell lines: *Lama2*-deficient, *p53*-deficient and *Lama2/p53*-deficient. For that, two different gRNAs were designed to target *Lama2* and another two to target *p53*, each of them expressing one gRNA that targets a specific site of the targeted gene – *Lama2*: exon 4 and 9; p53: exon 4 and 5. The gRNAs for exon 4 and 9 of *Lama2* and exon 4 of *p53* were commercial and the gRNA p53 exon 5 was designed in the laboratory. Colony PCR was performed to confirm that the gRNA was incorporated into the vector and the gel reveals that the gRNA targeting *p53* exon 5 incorporated (Figure 3.3 A). After puromycin selection, the pool of cells from each group was collected and the expression of *Lama2* and *p53* or both was analyzed by RT-qPCR. Analysis of *Lama2* expression revealed that the *Lama2* ko pool had a deletion of 80,28% and the *Lama2/p53* ko pool ~80%, compared to the wildtype (Wt) cells (Figure 3.3B, upper panel). Analysis of *p53* expression showed that *p53* ko pool had 88,85% deletion and *Lama2/p53* ko pool 93,8% (Figure 3.3 B, lower panel). Thus showing that CRISPR/Cas9 was successfully used, which is in line with previous results where C2C12 knockouts cell lines were generated with this system[78]. In order to obtain cell lines that where efficiently deleted for the target genes, single cell clones were established by limiting dilution cloning. Cells were then collected and analyzed using RT-qPCR. The schematic representation of the procedure is described in Figure 3.3 A.

As observed, several clones of *Lama2* single knockout (*Lama2* ko), *p53* single knockout (*p53* ko) and double *Lama2* and *p53* knockouts (dko) were obtained (Figure 3.3 B). Several clones obtained showed a decreased, but evident expression of *Lama2* and *p53* compared to the Wt, so they were used as knockdown models. The clones that had high expression levels of the targeted genes were discarded. Based on expression levels two *Lama2* ko clones (ko5 and ko6), two of the *p53* ko clones (p53 ko D and p53 ko G) and two of the double *Lama2/p53* ko clones (dko C and dko I) were selected for further analysis. (Figure 3.3 C).

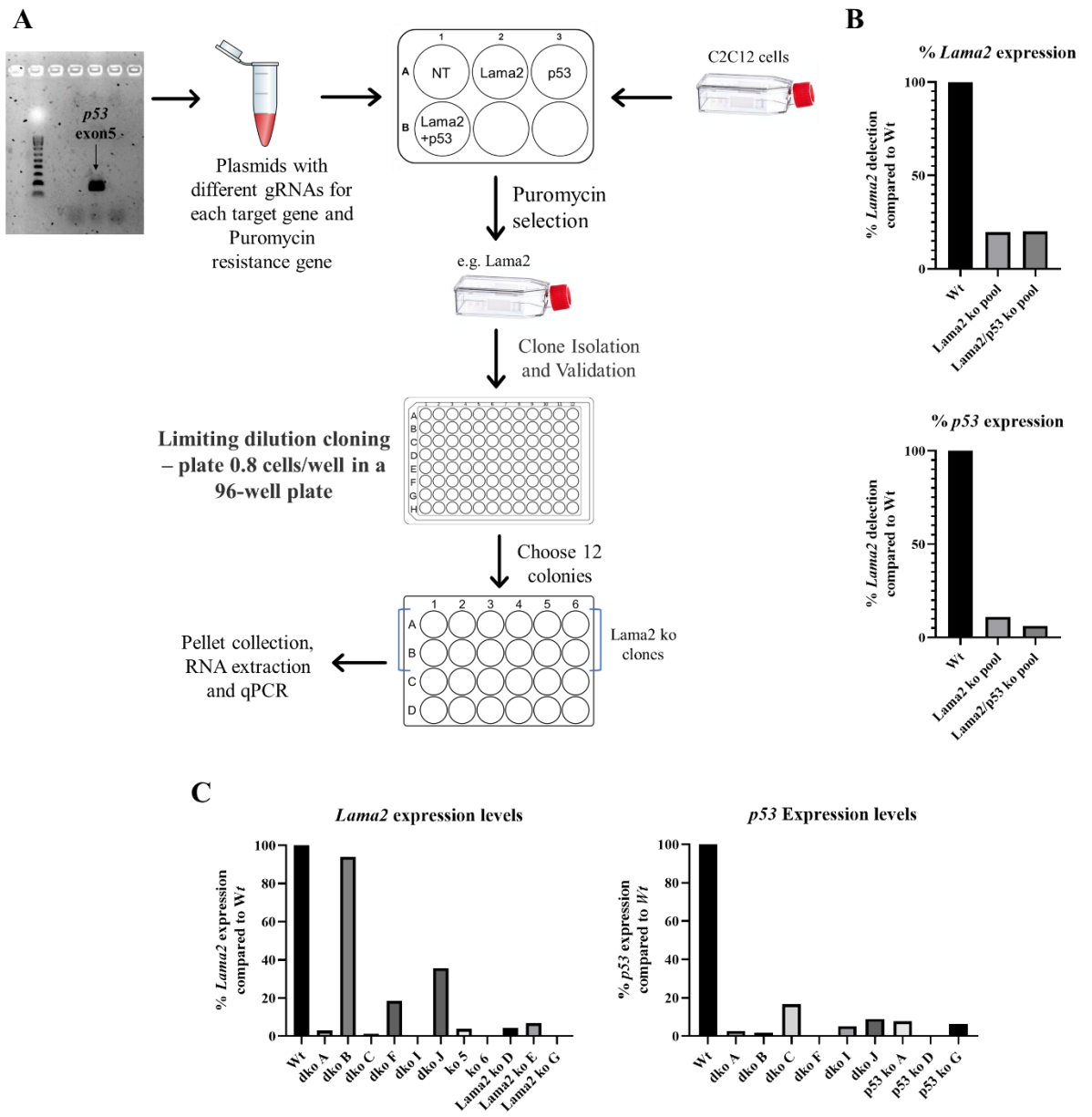

Figure 3.3 Generation of C2C12 myoblast cell lines deficient for *Lama2* and/or p53 as an *in vitro* system. (A) CRISPR-CAS9 was applied to C2C12 myoblast cells to obtain *Lama2* knockout clones (model for Lama2-CMD), using gRNA-Cas9 plasmids with different oligo sequences, that cut the target sequence in 2 different places to guarantee a successful knockout of the target gene. (B) After puromycin selection, the different pool groups were analyzed to calculate *Lama2* and *p53* expression to determine transfection efficiency. (C) Distinct clones were obtained: double knockouts of *Lama2* and *p53* (dko); single *Lama2* knockouts (Lama2 ko); and single *p53* knockouts (p53 ko). The quantification of *Lama2* and *p53* expression was done by Real-Time qPCR and normalized using the housekeeping gene Arbp0 expression. To calculate the percentage of *Lama2* and *p53* expression, the expression levels obtained by Real-Time qPCR were dived by the expression of wildtype cells for the respective genes.

Lama2 deficiency impacts on proliferation and cell cycle regulation

According to the *in vivo* analysis in Figure 3.1 A, we observed that dyW mice showed alterations in terms of the expression of genes linked to proliferation and cell cycle regulation. To further evaluate the impact of *Lama2* deficiency on cell proliferation and understand if C2C12 cells can be used as a model to study LAMA2-CMD disease, several experiments were performed to compare wt and *Lama2* ko C2C12 cells.

First, two genes linked to proliferation/quiescence that showed significant expression differences in dyW compared to wt fetuses were selected – *Cdkn1a* and *Mki67* (Figure 3.1 A). Analysis of *Mki67* and *Cdkn1a* expression by RT-qPCR was performed comparing the selected *Lama2*-deficient clones ko5 and ko6 and wt C2C12 cells. *Lama2* expression was also quantified once again to guarantee that even after the expansion, these clones were *Lama2*-deficient (Figure 3.4 A). *Lama2* expression was significantly decreased for both clones ko5 and ko6, compared to Wt C2C12 cells. The expression of *Cdkn1a* was decreased for ko5 and ko6, being more evident for the ko5, in contrast to the results obtained *in vivo*. For *Ki67*, only ko6 showed a tendency to be decreased compared to Wt cells, but ko5 showed a similar expression to Wt. The results obtained suggest that the *Lama2*-deficient C2C12 cell lines do not seem to have the same tendency as observed *in vivo*, in particular for the expression of *Cdkn1a*.

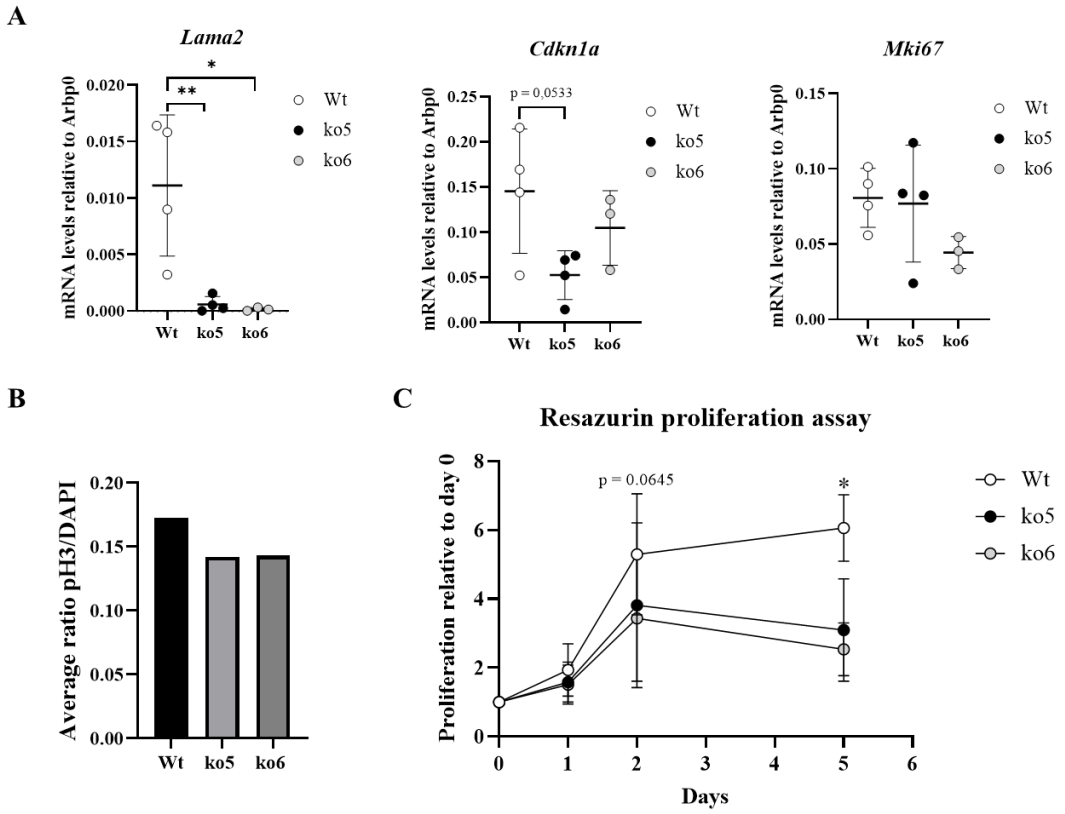

Figure 3.4 Reduced expression of *Lama2* decreases cell proliferation *in vitro*. (A) Wt, ko5 and ko6 cells were harvested on three independent days and RNA was extracted, followed by quantification of *Lama2*, *Cdkn1a* and *Mki67* expression by RT-qPCR and normalized using Arbp0 as housekeeping gene. Statistical analysis was performes using ordinary one-way Anova test. (B) Immunofluorescence was performed in C2C12 Wt, ko5 and ko6 cells. Cells were seeded on coverslips and immunostained for phospho-histone 3 (pH3) and counterstained for DNA (DAPI). Images were acquired using a fluorescence microscope. The number of cells stained with DAPI and pH3 was analyzed in three different fields, randomly acquired. The ratio was obtained dividing the average of cells stained with pH3 by the average of cells stained with DAPI. Graph shows the data from two independent experiments. (C) C2C12 Wt, ko5 and ko6 – were plated and cell proliferation was monitored on day 0, 1, 2 and 5 days using Resazurin. Data was plotted relative to day 0, in order to analyze proliferation rate. n = 3 independent experiments done with 4 technical replicates each. Statistical analysis was performes with student t-test. Bar = standard error. P-value: * $p<0.05$; ** $p<0.01$.

In order to understand the impact of *Lama2*-deficiency on C2C12 proliferation the number of phospho-histone 3 (pH3) positive cells, which is a marker for late G2/M phase, corresponding to cells undergoing mitosis, was analyzed by immunofluorescence in Wt *versus Lama2*-deficient cells. Wt, ko5 and ko6 C2C12 cell lines were immunostained for pH3 and counterstained with DAPI, in order to identify the total number of nuclei. Three randomly acquired fields were used to determine the number

of cells stained for DAPI and pH3. The ratio was obtained by dividing the average of cells stained with pH3 by the average of cells stained with DAPI (Figure 3.4 B). The results demonstrate a decreased pH3/DAPI ratio in *Lama2* ko cells, revealing a tendency for them to proliferate less.

To further validate these results, proliferation analysis was performed using the Resazurin assay. Resazurin is a compound (non-fluorescent) that is reduced to Resofurin (highly fluorescent) in the presence of metabolic active cells (viable cells), by the activity of several dehydrogenases. The amount of Resofurin produced is proportional to the number of viable cells and it is quantified by measuring the relative fluorescence emitted – more viable cells, more Resofurin and, consequently, increased fluorescence. It was also noticed the color change of the media over the days, revealing the conversion of Resazurin (blue) to Resofurin (pink). Fluorescence was measured on days 0, 1, 2 and 5. To analyze the proliferation rate, fluorescence values were normalized to day 0 (Figure 3.4 C). At day 1, the results showed no significant differences in terms of Resofurin fluorescence for all the cells, with only a slight tendency of Wt cells to be increased. At day 2, ko5 and ko6 had a similar behavior, showing a decreased Resofurin fluorescence compared to the Wt ($p = 0{,}0645$), suggesting less proliferation. Finally, at day 5, Wt proliferation Resofurin fluorescence levels begin to stabilize and remained similar to day 2, unlike clones ko5 and ko6, which demonstrate significant reduction in Resofurin fluorescence at day 5 compared to the Wt. Between day 2 and 5, ko5 and ko6 fluorescence reduction may indicate that cells start to die.

In order to understand if the reduction in the number of pH3 positive cells and decreased proliferation was due to an impairment in cell cycle progression, cell cycle analysis was performed by flow cytometry. For that, cells were stained with propidium iodide (PI), which is a fluorescent dye that is capable to intercalate into double stranded nucleic acids. PI binds in proportion to the amount of DNA present in the cell. The DNA quantity increases during the progression of mitosis, being the minimum in the G1 phase, followed by the S phase and reaching the maximum in the G2/mitosis phase. The higher the amount of DNA in each cell is, the greater the amount of fluorescence emitted (G1<S<G2/M).

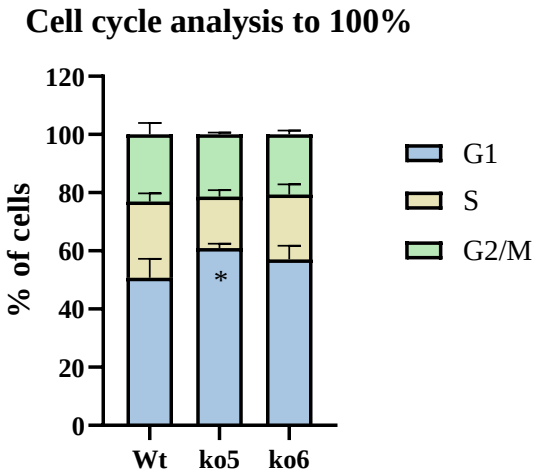

Figure 3.5 *Lama2*-deficiency induces cell cycle arrest at G1/G0. Flow cytometry analysis of Wt, ko5 and ko6 C2C12 cells stained with propidium iodide (PI) to quantify the number of cells in G1/G0, S and G2/M cell cycle phase. Statistical analysis was done using two-way ANOVA. Bar = standard error. P-value: * $p<0.05$; ** $p<0.01$. n = 2-3 experiments per cell line.
.

Flow cytometry analysis of cell cycle profiles show that for ko5 there was a significant increase in the number of cells in G1/G0 phase and, although not significant, ko6 showed the same tendency, when compared to the Wt cells (Figure 3.5). This suggests that the absence of *Lama2* induces G1/G0 cell cycle phase arrest.

Reduced p53 expression ameliorates cell proliferation impairment in *Lama2*-deficient cells *in vitro*

Taking into account the role of p53 as a cell cycle regulator, reducing the expression of this cell guardian could possibly rescue the decreased proliferation observed in Figure 3.4 A for *Lama2*-deficient cells compared to Wt C2C12 cells. For that, Resazurin proliferation assay was applied once more using Wt C2C12 cells, ko5, ko6, dko C and dko I and p53 D cells, obtained through CRISPR (Figure 3.6 A, B). The results confirmed a decrease in proliferation of ko5 and ko6 cells and demonstrated similar proliferation levels between Wt and dko I cells (Figure 3.6 C). p53 D clone, as expected, had higher proliferation compared to the other cell lines.

Flow cytometry results showed that the number of cells in G1/G0 phase was again increased for ko5 and ko6, being significantly increased for ko6 compared to the Wt cells (Figure 3.6 D). The double ko cells demonstrated distinct behaviors. Even though both showed increased number of cells arrested at G1/G0 phase, dko I was significantly increased. Finally, p53 D clones had similar number of cells at G1/G0 phase compared to Wt, despite showing greater proliferation in the Resazurin assay. These results suggests that decreased *p53* expression improves cell proliferation in *Lama2*-deficient cells, even though the effect on cell cycle arrest remains to be further studied.

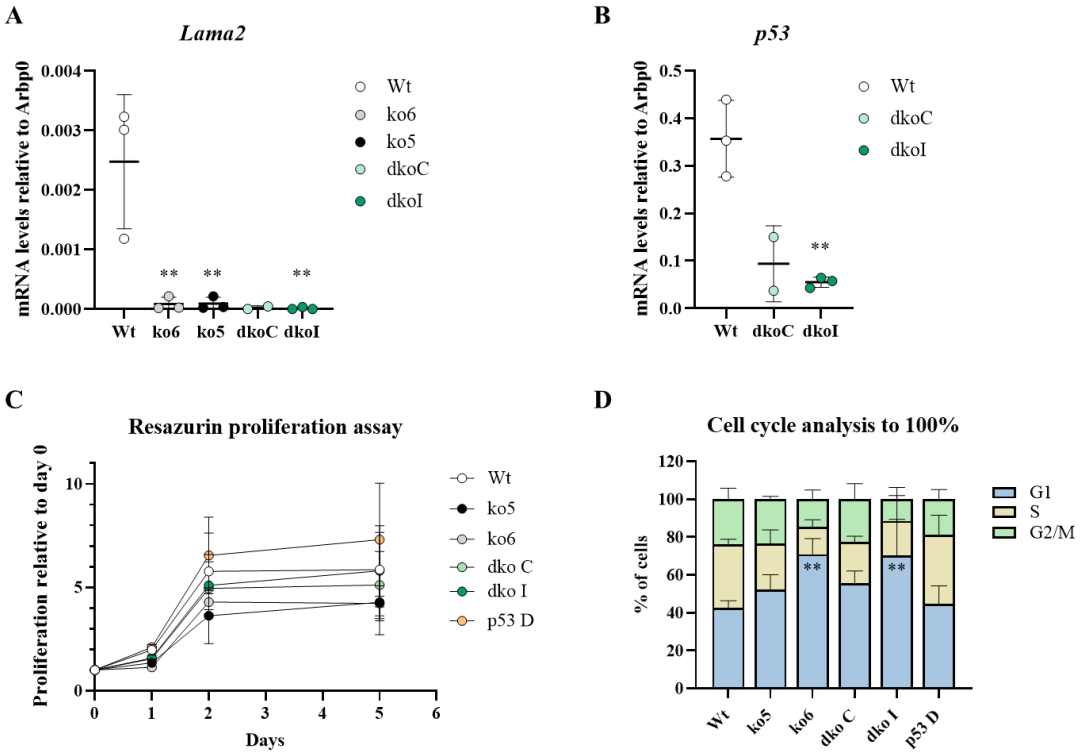

Figure 3.6 *p53* reduced expression rescues *Lama2* deficient C2C12 proliferation. (A, B) Cells were harvested on three independent days and RNA was extracted, followed by quantification of *Lama2* (A) and *p53* (B) expression by RT-qPCR and normalized using Arbp0 as housekeeping gene. Statistical analysis was performed using ordinary one-way Anova test, relative to Wt. (C) C2C12 Wt, ko5, ko6, dko C, dko I and p53 D cells – were plated and cell proliferation was monitored on day 0, 1, 2 and 5 days using Resazurin. Data was plotted relative to day 0, in order to analyze proliferation rate. n = 3 independent experiments done with 4 technical replicates each. (D) Flow cytometry analysis of Wt, ko5, ko6, dko C, dko I and p53 D C2C12 cells stained with propidium iodide (PI) to quantify the number of cells in G1/G0, S and G2/M cell cycle phase. Statistical analysis was done using two-way ANOVA. Bar = standard error. P-value: * $p<0.05$; ** $p<0.01$. n = 2-3 experiments per cell line.

Chapter 4 Discussion

LAMA2-CMD disorder is caused by mutations in *LAMA2*, a gene coding α2 subunit of laminin-211. Using the dyW mouse model for LAMA2-CMD the host laboratory showed that the onset of this disease occurs *in utero*, between E17.5 and E18.5, and is characterized by significant changes like decreased MuSC pool and muscle fiber size and also overactivation of JAK-STAT pathway[19]. The exact

pathway underlying disease onset have not yet been established. Therefore, the aim of this project was to address different cell cycle and survival pathways that may be altered in the absence of *LAMA2*, through the analysis of the expression of genes and proteins involved in these pathways, using deep back muscles of wt and dyW mice at E17.5 and E18.5. Another goal was to establish an *in vitro* model for LAMA2-CMD. This model aims at replacing *in vivo* and *ex vivo* models for the analyses of MuSCs, because the collection and isolation process of MuSC from mice proves to be complex and time-consuming and, having an *in vitro* model, also reduces the use of animals. To generate this *in vitro* model of LAMA2-CMD, *Lama2* mutations were generated in C2C12 myoblasts using CRISPR/Cas9, thus obtaining *Lama2*-deficient C2C12 cells. Since p53 is a protein that, as a transcription factor, is involved and triggers multiple cell fate pathways, including some that occur during myogenesis, *p53* and *Lama2/p53* knockout C2C12 cells were also generated. By studying *Lama2* mutations combined with *p53* mutations, we aimed to analyze if *p53* deletion was able to improve the phenotype associated with the absence of this laminin subunit.

To dissect the role of cell cycle and cell survival in the onset of LAMA2-CMD, different pathways were analyzed *in vivo* in dyW mice (Figure 3.1) and *in vitro* using *Lama2*-deficient C2C12 cells (Figure 3.4 A). Analysis of the expression of genes linked to proliferation/quiescence in fetal muscles showed a significant increase in the expression of *Cdkn1a* (p21) and *Cdkn1c* (p57) at E17.5 and *Cdkn1a* upregulation at E18.5, although not significant (p= 0,1263) (Figure 3.1 A). This suggests that there is an increase in cell cycle arrest. Moreover, using *p21*$^{-/-}$ mice, it was previously shown that p21 regulates cell cycle arrest of myoblasts during myogenesis, inducing them to stop proliferating and start differentiating to form fusion-competent myoblasts that fuse with myofibers, indicating that p21 is important for proper myogenesis[79,80]. However, increased expression of this gene can result in excessive and faster cell cycle arrest and decreased proliferation, which may explain the decrease in the number of MuSCs and myoblasts during the onset of the disease[19]. In accordance with this, *Mki67*, a marker present in all active phases of the cell cycle, but not in G0, was significantly downregulated at E18.5 in dyW muscles (Figure 3.1 A), suggesting an increase in the number of non-proliferative cells and that possibly there are more cells arrested in G0 phase in dyW comparing to wt muscles. This analysis also identified a significantly increased expression of *Pim1* at E17.5, results that are in agreement with previous studies[19] and likely associated with an overexpression of JAK-STAT3 pathway. However, this was not observed for E18.5. Although the expression of *Pim1* was not increased in dyW muscle at E18.5, an even more significantly increased phosphorylation of STAT3 was reported to occur in PN2 dyW mice[19], possibly suggesting that there is another mechanism enhancing this increased activation.

To analyze if *Lama2*-deficient C2C12 cell line can be used as a model of MuSCs and this way allow for the study of the mechanisms underlying LAMA2-CMD, several analyses were performed (Figures 3.4 to 3.7). Analysis of two genes that were differentially expressed *in vivo* (*Cdkn1a* and *Mki67*) comparing dyW and wt mice, show that *Cdkn1a* was downregulated for both ko5 and ko6 and *Mki67* expression of ko6 cells was decreased but ko5 was similar to Wt cells. The results for *Cdkn1a* were not expected, as they were the opposite of the ones *in vivo* (Figure 3.4A). Since *Lama2*-deficiency likely decreases proliferation[81] one would expect *Cdkn1a*/p21 expression to be increased, as it induces cell cycle arrest, and *Mki67* expression to be decreased. *Cdkn1a* was downregulated in both ko clones compared to the Wt cells (Figure 3.4 A), which is the opposite of the *in vivo* observations (Figure 3.1 A). However, it was possible to observe that both clones proliferated less than Wt cells. A possible explanation for this could rely on the complex role of p21 in the cell cycle[82]. Although p21 reduction is normally expected to increase cell proliferation, there are cases in which that does not happen. Transient induction of p21 can promote cell cycle progression by acting as an assembly factor of cyclin D-cdk4/cdk6[82]. In this case, p21 decrease leads to cell cycle impairment. As for *Mki67*, ko6 had a decrease in the expression of this gene (Figure 3.4 A), which is in agreement with the *in vivo* results (Figure 3.1 A), but the ko5 clone has a similar expression compared to the Wt. It is important to highlight that these

cells were analyzed in a state of proliferative myoblasts, more similar to MuSCs, so we cannot directly compare the results from *in vivo* and *in vitro*, as the *in vivo* ones reflect the gene expression of the whole muscle, which is mainly composed by totally differentiated myofibers. This comparison can possibly be done by letting the C2C12 cells differentiate to form myotubes and analyze the gene expression also at this point. The current study hence supports the idea that a reduction in *Cdkn1a*/p21 expression, together with *Mki67* expression, may indicate less proliferation. In agreement with this, immunostaining with pH3 (Figure 3.4 B) and Resazurin proliferation assay (Figure 3.4 C) showed a decreased proliferation of *Lama2*-deficient cells comparing to Wt cells. Complimentary analysis done using flow cytometry showed that a possible reason for the decreased proliferation was cell cycle arrest since the results demonstrated an increase of ko cells at G1/G0 phase compared to Wt, this difference being significant for ko5 (Figure 3.5), suggesting that *Lama2*-deficiency may lead to G1/G0 arrest.

Under homeostatic conditions, p53 is constantly being degraded, however, upon an insult, p53 is stabilized and activated, which regulates different pathways. This transcription factor, known to trigger cell cycle arrest (eg. through induction of *Cdkn1a*/p21 expression and G1 phase arrest)[83], was shown to be increased and accumulated in the nuclei of human LAMA2-CMD myogenic cells and *Lama2*$^{-/-}$ mice[69], which goes in line with the increase in the expression levels of p53 in fetal skeletal muscle at E18.5 (FIG 3.2 C). This suggests that decreased *p53* expression could rescue the impaired proliferation observed in *Lama2*-deficient conditions. p53 role in this context was evaluated by *p53* deletion combined with *Lama2*-deficiency (dko), in C2C12 cells. Using the Resazurin proliferation assay, the results showed an improvement in cell proliferation for dko clones, being similar to the Wt (Figure 3.6 C). Flow cytometry analysis performed with these cells exhibited increased number of cells arrested at G1/G0 phase. This result was not expected, as dko I had lower p53 expression than dko C (Figure 3.3 C) and that rescue on proliferation defect was more notorious for dko I than dko C, even though both showed improvements, possibly revealing that partial p53 reduction could be more beneficial. Although not expected, this could be explained by the fact that different levels of p53 lead to different outcomes[62]. However, to fully understand these results, cell synchronization experiments are required. Here, reagents that block all the cell lines at the same cell cycle phase are used, normally at G1 or M phase, and then released to follow cycle progression.

Analysis of autophagy related genes *in vivo* showed that expression of *Lamp2a* at E18.5 was similar between dyW and wt but *Atg7* gene expression was significantly increased, revealing a possible activation of autophagy (Figure 3.1 C). Consistent with this, a study using the dy3k mouse model of LAMA2-CMD, showed that increased autophagy is a characteristic of LAMA2-CMD, and that some genes linked to this mechanism were upregulated in a postnatal context[70]. In addition, absence of laminin-211 in dy3k mice was previously correlated with autophagy-lysosome pathway overactivation[22]. Data presented here, suggests that the onset of autophagy deregulation in dyW muscles may occur already during embryonic development, around E18.5.

Even though apoptosis is a typical hallmark in several muscular dystrophies, including LAMA2-CMD, this process is not increased in muscles during embryonic development[19]. These results are in agreement with ours, as *Bax* and *Bcl2* expression values were not significantly altered compared to wt mice (Figure 3.1 B). Apoptosis is only significant postnatally when there is a considerable damage accumulation. Thus, it is likely that increased apoptosis is not the reason for the decrease in MuSCs and reduced myofiber size, in accordance with previous results[19]. Although there is a close relationship between autophagy and apoptosis, autophagy can either act together with apoptosis and induce cell death or against it. The results were not conclusive about this connection.

Senescence is characterized by the expression of SASPs, which include secretion of several inflammatory cytokines and interleukins. Ccl family members can appear upregulated in senescent cells. For that reason, *Ccl7* gene, coding for the chemokine (C-C motif) ligand 7 (CCL7), was assessed and it was significantly upregulated in dyW mice (Figure 3.1 D), suggesting that senescence may be prevalent

in this genotype. *Il-6ra*, coding for *Il-6* receptor alpha chain, is expressed by several immune cells and several tissues, including skeletal muscle. Il-6 ligation to these receptors induces signal transduction and transcription of several cytokines, thus mediating an inflammatory response and promoting cell senescence by playing a role in the senescence-associated secretory phenotype. Il-6r is a receptor that activates JAK-STAT3 pathway, leading to either myoblast proliferation and premature differentiation prevention or myogenic differentiation, depending on the activated JAK protein[66,84]. At E17.5 *Il-6ra* expression showed a tendency to be increased in dyW mice (p=0,0943) but at E18.5 mRNA expression was similar for both genotypes (Figure 3.1 D). STAT3 phosphorylation levels in dyW revealed a tendency to be increased compared to the wt, even though it was not significant (Figure 3.2 A,B), in accordance with previous results. So, Il-6ra may contribute to increased activation of JAK-STAT. JAK-STAT3 overactivation was shown to be a characteristic of aged MuSCs which display impaired muscle regeneration and has also been implicated in promoting asymmetric MuSCs divisions[19,68,85]. It is possible that laminin-211 controls STAT3 activation and prevents JAK-STAT3 overactivation and favors symmetric divisions in order to maintain the pool of Pax7-positive MuSCs[19]. Moreover, JAK-STAT3 overactivation is known to promote MyoD expression[19,86], which induces cell cycle arrest through p21 induction[87]. Our *in vivo* RT-qPCR results show increased *Cdkn1a* expression and we see impaired proliferation, which together may explain the decreased number of MuSCs, resulting in fewer myogenic cells. Although the connection between LAMA2-CMD and senescence has not been established, chronic cellular senescence was shown to exacerbate Duchenne muscular dystrophy and the inhibition of senescence improved disease pathology[88]. Increased expression Ccl7 and Il-6ra, would be expected to increase inflammation in the dyW muscles. However, Nunes et al. showed that neither inflammation nor fibrosis were augmented at E17.5 or PN2.

Overall, cell cycle arrest seems to be increased, either from *Cdkn1a* and *Cdkn1c* upregulation and *Mki67* downregulation, and this arrest is characteristic for the other mechanisms, especially quiescence, senescence and apoptosis. This is further supported by the data *in vitro*. Although there was no difference in apoptosis related genes, one out of the two senescence related genes analyzed, was upregulated. The increased expression of the autophagy related gene may reveal an effort of the cells to maintain the metabolic needs and possibly control increased levels of reactive oxygen species (ROS), another characteristic of LAMA2-CMD patients[24,10]. So, one possibility is that autophagy increases to oppose ROS, thus leading to decreased metabolic activity and consequently decreased proliferation, either by entry into quiescence or senescence.

Although so far there is no cure or efficient approved treatments for LAMA2-CMD, several studies with different experimental therapies are ongoing[89]. This includes the expression of *Lama1* to substitute *Lama2* using CRISPR/dCas9 technology in mice[90] or the injection of laminin-111 or laminin-211[91]. Since laminin-111 is structurally similar to laminin-211, supplementation with laminin-111 was shown to improve the activity of null-*Lama2* mice and promotes muscle repair by satellite stem cell activation but results in the depletion of this pool. Laminin-211 supplementation increases and preserves the stem cell pool but decreases the number of myogenic-positive cells. So, a combination of these two laminin supplements could possibly maximize the treatment[91]. Several therapies target secondary alterations instead of the primary cause of this disease, including autophagy[70,92] and apoptosis inhibition ameliorated several symptoms associated with LAMA2-CMD[93,94,95]. Currently, an anti-apoptotic drug (omigapil) is under phase I of clinical trials, used to evaluate its safety and tolerability for CMD treatments[96,97].

Increased activation of JAK-STAT and increased expression of p53 may play a role in LAMA2-CMD onset and subsequent progression, by altering several pathways linked to cell cycle arrest and progression, autophagy and senescence. Our results show the importance of developing prenatal diagnosis for this disorder to intervene as soon as possible by applying *in utero* therapies that target differentially expressed genes during fetal muscle development. By decreasing JAK-STAT

overactivation by reduction of STAT3 activation during MuSCs niche formation underneath myofiber BM (E17.5 in mice), symmetrical divisions might be promoted in order to increase the pool of these stem cells, which is crucial for correct muscle development and regeneration. If prenatal diagnosis proves difficult, targeting MuSCs soon after birth may also ameliorate symptoms and disease progression.

In vivo results indicated an increase in genes linked to quiescence, senescence and autophagy, which can be involved in decreased proliferation and, consequently, decreased muscle size. *In vitro* analysis of C2C12 *Lama2*-deficient myoblasts reinforced this notion and suggested that the impaired proliferation in these cells may be linked to G1/G0 cell cycle arrest, which may also occur *in vivo* and therefore cause a reduction in the MuSCs pool. As p53 inhibition was previously referred as possible therapy to reduce apoptosis, in this context p53 can be used to enhance proliferation of the MuSCs[98].

This hypothesis can be tested in the future using dyW/p53$^{-/-}$ mice. Analysis of the double knockout mice will allow to determine if p53 knockout is required and sufficient to ameliorate phenotypic hallmarks of this disease. The different C2C12 *Lama2*-deficient cell lines generated in this project can be further analyzed as an alternative model to study MuSCs of LAMA2-CMD. This will allow to understand if differentiation of C2C12 cells into myotubes is also affected by *Lama2*-deficiency and could be used as an *in vitro* model of LAMA2-CMD to study more deeply the mechanism altered by *Lama2*-deficiency without the need to sacrifice animals.

Overall, this work brought knowledge on how the absence of *Lama2* impacts and alters mechanisms involved in cell fate during the onset of LAMA2-CMD during mouse fetal development. Being the most common congenital muscular, a better understanding of the mechanisms that trigger the appearance of this condition is crucial to develop therapeutical approaches that can prolong the lifespan and increase the wellbeing of patients.

Chapter 5 Bibliography

1. Frantz, C., Stewart, K. M. & Weaver, V. M. The extracellular matrix at a glance. *Journal of Cell Science* vol. 123 (2010).

2. Thorsteinsdottir, S., Deries, M., Cachaço, A. S. & Bajanca, F. The extracellular matrix dimension of skeletal muscle development. *Developmental Biology* vol. 354 (2011).

3. Lamandé, S. R. & Bateman, J. F. Genetic Disorders of the Extracellular Matrix. *Anatomical Record* 303, (2020).

4. Rozario, T. & DeSimone, D. W. The extracellular matrix in development and morphogenesis: A dynamic view. *Developmental Biology* vol. 341 (2010).

5. Yanagishita, M. Function of proteoglycans in the extracellular matrix. *Pathology International* vol. 43 (1993).

6. Kruegel, J. & Miosge, N. Basement membrane components are key players in specialized extracellular matrices. *Cellular and Molecular Life Sciences* vol. 67 (2010).

7. Paulson, M. Basement membrane proteins: Structure, assembly, and cellular interactions. *Critical Reviews in Biochemistry and Molecular Biology* 27, (1992).

8. Yurchenco, P. D., McKee, K. K., Reinhard, J. R. & Rüegg, M. A. Laminin-deficient muscular dystrophy: Molecular pathogenesis and structural repair strategies. *Matrix Biology* vols. 71–72 (2018).

9. Yurchenco, P. D., Amenta, P. S. & Patton, B. L. Basement membrane assembly, stability and activities observed through a developmental lens. *Matrix Biology* 22, (2004).

10. Martins, S. G., Zilhão, R., Thorsteinsdóttir, S. & Carlos, A. R. Linking Oxidative Stress and DNA Damage to Changes in the Expression of Extracellular Matrix Components. *Frontiers in Genetics* vol. 12 (2021).

11. Hohenester, E. & Yurchenco, P. D. Laminins in basement membrane assembly. *Cell Adhesion and Migration* vol. 7 (2013).

12. Yousif, L. F., di Russo, J. & Sorokin, L. Laminin isoforms in endothelial and perivascular basement membranes. *Cell Adhesion and Migration* vol. 7 (2013).

13. Tanjore, H. & Kalluri, R. The role of type IV collagen and basement membranes in cancer progression and metastasis. *American Journal of Pathology* vol. 168 (2006).

14. Dai, J. *et al.* Dissection of Nidogen function in Drosophila reveals tissue-specific mechanisms of basement membrane assembly. *PLoS Genetics* 14, (2018).

15. Deries, M., Gonçalves, A. B. & Thorsteinsdóttir, S. Skeletal Muscle Development: From Stem Cells to Body Movement. in (2020). doi:10.1007/978-3-030-43939-2_9.

16. Petrof, B. J., Shrager, J. B., Stedman, H. H., Kelly, A. M. & Sweeney, H. L. Dystrophin protects the sarcolemma from stresses developed during muscle contraction. *Proceedings of the National Academy of Sciences of the United States of America* 90, (1993).

17. Durbeej, M. Laminin-α2 Chain-Deficient Congenital Muscular Dystrophy. Pathophysiology and Development of Treatment. *Current Topics in Membranes* 76, (2015).

18. Carter, J. C., Sheehan, D. W., Prochoroff, A. & Birnkrant, D. J. Muscular Dystrophies. *Clinics in Chest Medicine* vol. 39 (2018).

19. Nunes, A. M. *et al.* Impaired fetal muscle development and JAK-STAT activation mark disease onset and progression in a mouse model for merosin-deficient congenital muscular dystrophy. *Human Molecular Genetics* 26, (2017).

20. Fontes-Oliveira, C. C., Steinz, M., Schneiderat, P., Mulder, H. & Durbeej, M. Bioenergetic Impairment in Congenital Muscular Dystrophy Type 1A and Leigh Syndrome Muscle Cells. *Scientific Reports* 7, (2017).

21. Gawlik, K. I. & Durbeej, M. Skeletal muscle laminin and MDC1A: pathogenesis and treatment strategies. *Skeletal Muscle* vol. 1 (2011).

22. Sarkozy, A., Foley, A. R., Zambon, A. A., Bönnemann, C. G. & Muntoni, F. LAMA2-Related Dystrophies: Clinical Phenotypes, Disease Biomarkers, and Clinical Trial Readiness. *Frontiers in Molecular Neuroscience* vol. 13 (2020).

23. Holmberg, J. & Durbeej, M. Laminin-211 in skeletal muscle function. *Cell Adhesion and Migration* vol. 7 (2013).

24. Harandi, V. M. *et al.* Antioxidants reduce muscular dystrophy in the dy2J/dy2J mouse model of laminin α2 chain-deficient muscular dystrophy. *Antioxidants* 9, (2020).

25. Oliveira, J. *et al.* LAMA2 gene mutation update: Toward a more comprehensive picture of the laminin-α2 variome and its related phenotypes. *Human Mutation* 39, (2018).

26. Mendell, J. R., Boué, D. R. & Martin, P. T. The congenital muscular dystrophies: Recent advances and molecular insights. *Pediatric and Developmental Pathology* vol. 9 (2006).

27. Rooney, J. E., Knapp, J. R., Hodges, B. L., Wuebbles, R. D. & Burkin, D. J. Laminin-111 protein therapy reduces muscle pathology and improves viability of a mouse model of merosin-deficient congenital muscular dystrophy. *American Journal of Pathology* 180, (2012).

28. Patton, B. L., Miner, J. H., Chiu, A. Y. & Sanes, J. R. Distribution and function of laminins in the neuromuscular system of developing, adult, and mutant mice. *Journal of Cell Biology* 139, (1997).

29. Guo, L. T. *et al.* Laminin α2 deficiency and muscular dystrophy; genotype-phenotype correlation in mutant mice. *Neuromuscular Disorders* 13, (2003).

30. Kuang, W. *et al.* Merosin-deficient congenital muscular dystrophy: Partial genetic correction in two mouse models. *Journal of Clinical Investigation* 102, (1998).

31. Gawlik, K. I. & Durbeej, M. A Family of Laminin α2 Chain-Deficient Mouse Mutants: Advancing the Research on LAMA2-CMD. *Frontiers in Molecular Neuroscience* vol. 13 (2020).

32. Deries, M. & Thorsteinsdóttir, S. Axial and limb muscle development: dialogue with the neighbourhood. *Cellular and Molecular Life Sciences* vol. 73 (2016).

33. Chal, J. & Pourquié, O. Making muscle: Skeletal myogenesis in vivo and in vitro. *Development (Cambridge)* vol. 144 (2017).

34. Bajanca, F. *et al.* Integrin α6β1-laminin interactions regulate early myotome formation in the mouse embryo. *Development* 133, (2006).

35. Anderson, C., Thorsteinsdóttir, S. & Borycki, A. G. Sonic hedgehog-dependent synthesis of laminin α1 controls basement membrane assembly in the myotome. *Development* 136, (2009).

36. Bentzinger, C. F., Wang, Y. X. & Rudnicki, M. A. Building muscle: molecular regulation of myogenesis. *Cold Spring Harbor perspectives in biology* vol. 4 (2012).

37. Matsakas, A., Otto, A., Elashry, M. I., Brown, S. C. & Patel, K. Altered primary and secondary myogenesis in the myostatin-null mouse. *Rejuvenation Research* 13, (2010).

38. Zammit, P. S. & Beauchamp, J. R. The skeletal muscle satellite cell: Stem cell or son of stem cell? *Differentiation* vol. 68 (2001).

39. Moresi, V., Adamo, S. & Berghella, L. The JAK/STAT pathway in skeletal muscle pathophysiology. *Frontiers in Physiology* vol. 10 (2019).

40. Hodges, B. L. *et al.* Altered expression of the α7β1 integrin in human and murine muscular dystrophies. *Journal of Cell Science* 110, (1997).

41. Gattazzo, F., Urciuolo, A. & Bonaldo, P. Extracellular matrix: A dynamic microenvironment for stem cell niche. *Biochimica et Biophysica Acta - General Subjects* vol. 1840 (2014).

42. Harper, J. v. & Brooks, G. The mammalian cell cycle: an overview. *Methods in molecular biology (Clifton, N.J.)* vol. 296 (2005).

43. Vermeulen, K., van Bockstaele, D. R. & Berneman, Z. N. The cell cycle: A review of regulation, deregulation and therapeutic targets in cancer. *Cell Proliferation* vol. 36 (2003).

44. Boya, P., Codogno, P. & Rodriguez-Muela, N. Autophagy in stem cells: repair, remodelling and metabolic reprogramming. *Development (Cambridge, England)* vol. 145 (2018).

45. Flamini, V. *et al.* The Satellite Cell Niche Regulates the Balance between Myoblast Differentiation and Self-Renewal via p53. *Stem Cell Reports* 10, (2018).

46. Wan, M., Gray-Gaillard, E. F. & Elisseeff, J. H. Cellular senescence in musculoskeletal homeostasis, diseases, and regeneration. *Bone Research* vol. 9 (2021).

47. Song, S., Lam, E. W. F., Tchkonia, T., Kirkland, J. L. & Sun, Y. Senescent Cells: Emerging Targets for Human Aging and Age-Related Diseases. *Trends in Biochemical Sciences* vol. 45 (2020).

48. van Deursen, J. M. The role of senescent cells in ageing. *Nature* vol. 509 (2014).

49. Saito, Y. & Chikenji, T. S. Diverse Roles of Cellular Senescence in Skeletal Muscle Inflammation, Regeneration, and Therapeutics. *Frontiers in Pharmacology* vol. 12 (2021).

50. Ritschka, B. *et al.* The senescence-associated secretory phenotype induces cellular plasticity and tissue regeneration. *Genes and Development* 31, (2017).

51. Sebastián, D. & Zorzano, A. Self-Eating for Muscle Fitness: Autophagy in the Control of Energy Metabolism. *Developmental Cell* vol. 54 (2020).

52. Mizushima, N. & Levine, B. Autophagy in mammalian development and differentiation. *Nature Cell Biology* vol. 12 (2010).

53. Zecchini, S. *et al.* Autophagy controls neonatal myogenesis by regulating the GH-IGF1 system through a NFE2L2- and DDIT3-mediated mechanism. *Autophagy* 15, (2019).

54. Xia, Q. *et al.* The Role of Autophagy in Skeletal Muscle Diseases. *Frontiers in Physiology* vol. 12 (2021).

55. Elmore, S. Apoptosis: A Review of Programmed Cell Death. *Toxicologic Pathology* vol. 35 (2007).

56. Wanner, E., Thoppil, H. & Riabowol, K. Senescence and Apoptosis: Architects of Mammalian Development. *Frontiers in Cell and Developmental Biology* vol. 8 (2021).

57. Childs, B. G., Baker, D. J., Kirkland, J. L., Campisi, J. & Deursen, J. M. Senescence and apoptosis: dueling or complementary cell fates? *EMBO reports* 15, (2014).

58. Brito Neto, E. P. de *et al.* Expression of apoptosis and myogenesis related genes during prenatal life in two divergent breeds of pigs. *Theriogenology* 145, (2020).

59. Chen, Q. J. *et al.* Apoptosis during the development of pelvic floor muscle in anorectal malformation rats. *Journal of Pediatric Surgery* 44, (2009).

60. Suzanne, M. & Steller, H. Shaping organisms with apoptosis. *Cell Death and Differentiation* vol. 20 (2013).

61. Sandri, M. & Carraro, U. Apoptosis of skeletal muscles during development and disease. *International Journal of Biochemistry and Cell Biology* 31, (1999).

62. Serrano, M. Shifting senescence into quiescence by turning up p53. *Cell Cycle* vol. 9 (2010).

63. Tasdemir, E. *et al.* Regulation of autophagy by cytoplasmic p53. *Nature Cell Biology* 10, (2008).

64. Garrido, C. *et al.* Mechanisms of cytochrome c release from mitochondria. *Cell Death and Differentiation* vol. 13 (2006).

65. Cerone, M. A. *et al.* p53 is involved in the differentiation but not in the differentiation-associated apoptosis of myoblasts. *Cell Death and Differentiation* vol. 7 (2000).

66. Jang, Y.-N. & Baik, E. J. JAK-STAT pathway and myogenic differentiation. *JAK-STAT* 2, (2013).

67. Chen, M. *et al.* Inhibition of JAK-STAT Signaling Pathway Alleviates Age-Related Phenotypes in Tendon Stem/Progenitor Cells. *Frontiers in Cell and Developmental Biology* 9, (2021).

68. Price, F. D. *et al.* Inhibition of JAK-STAT signaling stimulates adult satellite cell function. *Nature Medicine* 20, (2014).

69. Yoon, S. *et al.* Aberrant Caspase Activation in Laminin-α2-Deficient Human Myogenic Cells is Mediated by p53 and Sirtuin Activity. *Journal of Neuromuscular Diseases* 5, (2018).

70. Carmignac, V. *et al.* Autophagy is increased in laminin α2 chain-deficient muscle and its inhibition improves muscle morphology in a mouse model of MDC1A. *Human Molecular Genetics* 20, (2011).

71. Fontes-Oliveira, C. C., Steinz, M., Schneiderat, P., Mulder, H. & Durbeej, M. Bioenergetic Impairment in Congenital Muscular Dystrophy Type 1A and Leigh Syndrome Muscle Cells. *Scientific Reports* 7, (2017).

72. Hsu, P. D., Lander, E. S. & Zhang, F. Development and applications of CRISPR-Cas9 for genome engineering. *Cell* vol. 157 (2014).

73. Burattini, S. *et al.* C2C12 murine myoblasts as a model of skeletal muscle development: Morpho-functional characterization. *European Journal of Histochemistry* 48, (2004).

74. Yamauchi, J., Kumar, A., Duarte, L., Mehuron, T. & Girgenrath, M. Triggering regeneration and tackling apoptosis: A combinatorial approach to treating congenital muscular dystrophy type 1 A. *Human Molecular Genetics* 22, (2013).

75. Filomeni, G., de Zio, D. & Cecconi, F. Oxidative stress and autophagy: The clash between damage and metabolic needs. *Cell Death and Differentiation* vol. 22 (2015).

76. Guadagnin, E., Mázala, D. & Chen, Y. W. STAT3 in skeletal muscle function and disorders. *International Journal of Molecular Sciences* vol. 19 (2018).

77. Xu, Y. S. *et al.* STAT3 Undergoes Acetylation-dependent Mitochondrial Translocation to Regulate Pyruvate Metabolism. *Scientific Reports* 6, (2016).

78. Wang, L., Ma, S., Ding, Q., Wang, X. & Chen, Y. CRISPR/Cas9-mediated MSTN gene editing induced mitochondrial alterations in C2C12 myoblast cells. *Electronic Journal of Biotechnology* 40, (2019).

79. Hawke, T. J. *et al.* p21 is essential for normal myogenic progenitor cell function in regenerating skeletal muscle. *American Journal of Physiology - Cell Physiology* 285, (2003).

80. Yin, H., Price, F. & Rudnicki, M. A. Satellite cells and the muscle stem cell niche. *Physiological Reviews* 93, (2013).

81. Girgenrath, M., Kostek, C. A. & Miller, J. B. Diseased muscles that lack dystrophin or laminin-α2 have altered compositions and proliferation of mononuclear cell populations. *BMC Neurology* 5, (2005).

82. Gartel, A. L. & Radhakrishnan, S. K. Lost in transcription: p21 repression, mechanisms, and consequences. *Cancer Research* vol. 65 (2005).

83. Kagawa, S. *et al.* p53 expression overcomes p21WAF1/CIP1-mediated G1 arrest and induces apoptosis in human cancer cells. *Oncogene* 15, (1997).

84. Ward, N. L. Introduction to a special issue on Skin disease, immune response and cytokines. *Cytokine* vol. 73 (2015).

85. Yamakawa, H., Kusumoto, D., Hashimoto, H. & Yuasa, S. Stem cell aging in skeletal muscle regeneration and disease. *International Journal of Molecular Sciences* vol. 21 (2020).

86. Tierney, M. T. *et al.* STAT3 signaling controls satellite cell expansion and skeletal muscle repair. *Nature Medicine* 20, (2014).

87. Kataoka, Y. *et al.* Reciprocal Inhibition between MyoD and STAT3 in the Regulation of Growth and Differentiation of Myoblasts. *Journal of Biological Chemistry* 278, (2003).

88. Sugihara, H. *et al.* Cellular senescence-mediated exacerbation of Duchenne muscular dystrophy. *Scientific Reports* 10, (2020).

89. Packer, D. & Martin, P. T. Micro-laminin gene therapy can function as an inhibitor of muscle disease in the dyW mouse model of MDC1A. *Molecular Therapy - Methods and Clinical Development* 21, (2021).

90. Kemaladewi, D. U. *et al.* A mutation-independent approach for muscular dystrophy via upregulation of a modifier gene. *Nature* 572, (2019).

91. Barraza-Flores, P. *et al.* Human laminin-111 and laminin-211 protein therapy prevents muscle disease progression in an immunodeficient mouse model of LAMA2-CMD. *Skeletal Muscle* 10, (2020).

92. Carmignac, V., Quéré, R. & Durbeej, M. Proteasome inhibition improves the muscle of laminin α2 chain-deficient mice. *Human Molecular Genetics* 20, (2011).

93. Girgenrath, M., Dominov, J. A., Kostek, C. A. & Miller, J. B. Inhibition of apoptosis improves outcome in a model of congenital muscular dystrophy. *Journal of Clinical Investigation* 114, (2004).

94. Dominov, J. A. *et al.* Muscle-specific BCL2 expression ameliorates muscle disease in laminin α2-deficient, but not in dystrophin-deficient, mice. *Human Molecular Genetics* 14, (2005).

95. Erb, M. *et al.* Omigapil ameliorates the pathology of muscle dystrophy caused by laminin-α2 deficiency. *Journal of Pharmacology and Experimental Therapeutics* 331, (2009).

96. Foley, A. *et al.* CONGENITAL MUSCULAR DYSTROPHY: LAMA2: P.329CALLISTO: a phase I open-label, sequential group, cohort study of pharmacokinetics and safety of omigapil in LAMA2 and COL6-related dystrophy patients. *Neuromuscular disorders* 29, (2019).

97. Leach, M. *et al.* Congenital muscular dystrophy ascending multiple dose cohort study analyzing pharmacokinetics at three dose levels in children and adolescents with assessment of safety and tolerability of omigapil (CALLISTO) trial update. *Neuromuscular Disorders* 27, (2017).

98. Gudkov, A. v. & Komarova, E. A. Dangerous habits of a security guard: The two faces of p53 as a drug target. *Human Molecular Genetics* vol. 16 (2007).

Annexes

Table S1 List of primers used for genotyping.

	Primer	Sequence
p53	Dop53 Neo	5' CTA TCA GGA CAT AGC GTT 3'
	Dop53 WT	5' AAG CTA TTC TGC CAG CTG 3'
	Dop53 Rev	5' CTC ATA AGG TAC CAC CAC GC 3'
dyW	Primer 1	5' ACTGCCCTTTC TCACCCACCCTT 3'
	Primer 2	5' GTTGATGCGCTTGGGACTG 3'
	Primer 3	5' GTCGACGACGACAGTACTGGCCTCAG 3'

Table S2 PCR protocol for mice genotyping.

Cycling			
Step #	**Temp °C**	**Time**	**Note**
1	94	2 min	
2	94	20 sec	
3	65	15 sec	-0,5 °C per cycle decrease
4	68	10 sec	
5			Repeat steps 2-4 for 10 cycles
(Touchdown)			
6	94	15 sec	
7	60	15 sec	
8	72	10 sec	
9			Repeat steps 6-8 for 28 cycles
10	72	2 min	
11	12		Hold

Table S3 List of primers used for cell fate analyzes.

Gene	Primer	Sequence
Arbp0	Forward	5’ CTTTGGGCATCACCACGAA 3’
	Reverse	5’ GCTGGCTCCCACCTTGTCT 3’
Pim1	Pim_Ms_Forward	5’ AAGGGCCAAGTGTTCTTCAGGC 3’
	Pim_Ms_Reverse	5’ TTCCGGATTTCTTCAAAGGAGGGC 3’
p21	P21_Ms_Forward	5’ TGTCTGAGCGGCCTGAAGATT 3’
	P21_Ms_Reverse	5’ AAGACCAATCTGCGCTTGGAGT 3’
Bax	Forward	5’ AAACTGGTGCTCAAGGCCC 3’
	Reverse	5’ TTGGATCCAGACAAGCAGCC 3’
Lamp2a	Forward	5’ TGGCTAATGGCTCAGCTTTC 3’
	Reverse	5’ ATGGGCACAAGGAAGTTGTC 3’
Ccl7	Forward	5’ CCCTGGGAAGCTGTTATCTTCAA 3’
	Reverse	5’ CTCGACCCACTTCTGATGGG 3’
Cdkn1c	Forward	5’ GCCAATGCGAACGACTTCTT 3’
	Reverse	5’ ATCTCAGACGTTTGCGCGG 3’

Il-6ra	Forward	5’ GGAACCCCACACAGGTCTCT 3’
	Reverse	5’ CAGAGAAGCAACCCAAACGC 3’
Ki67	Ki67_Ms_Forward	5’ ATCCTGTCACTCCAGATCAGAACTC 3’
	Ki67_Ms_Reverse	5’ ATCCCGACATTCTCTGCAGATGC 3’
Atg7	Forward	5’ CAGAAGAAGTTGAACGAGTA 3’
	Reverse	5’ CAGAGTCACCATTGTAGTAAT 3’
Bcl2	Forward	5’ AACAGGGAGATGTCACCCCTGG 3’
	Reverse	5’ AGCCTCCGTTATCCTGGATCC 3’
Lama2	Forward	5’ TGAAAGCAAGGCCAGAAGTCA 3’
	Reverse	5’ ACAAAACCAGGCTTGGGGAA 3’
p53	Forward	5’ CTCCGAAGACTGGATGACTG 3’
	Reverse	5’ GCTTCACTTGGGCCTTCAAA 3’

Table S4 Real-Time PCR protocol used in CFX96™ system.

			Amplification			
Real-Time PCR System	**Setting/ Mode**	**Polymerase Activation and DNA Denaturation**	**Denaturation at 95°C/98°C**	**Annealing/Extension and Plate Read at 60°C**	**Cycles**	**Melt Curve Analysis**
Bio-Rad CFX96^{T}	SYBR only	30 sec at 95°C or 98°C for cDNA or 2-3 min at 98°C for genomic DNA	5-15 sec	15-30 sec	35-40	65-95°C; 0.5°C increments at 2-5 sec/step (or use instrument default setting)

Cdkn1a

E17.5

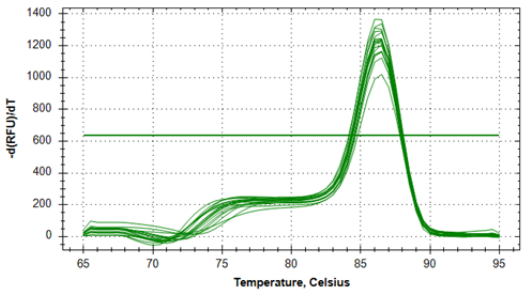

E18.5

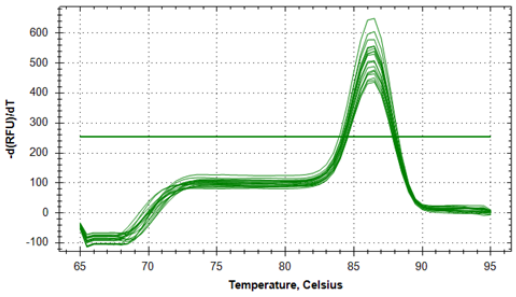

Cdkn1c

E17.5

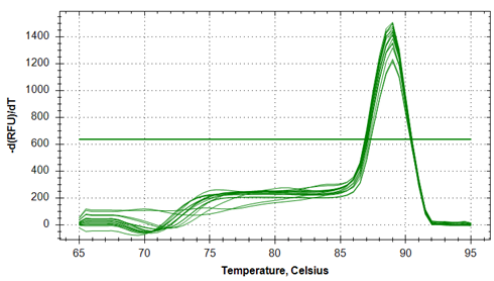

E18.5

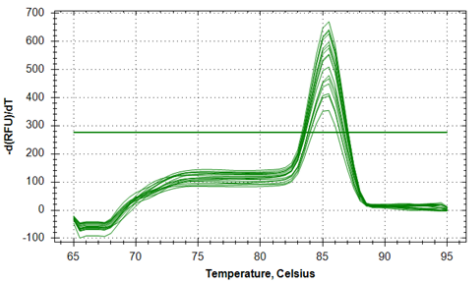

Pim1

E17.5

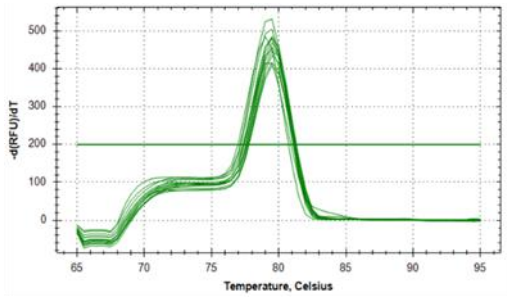

E18.5

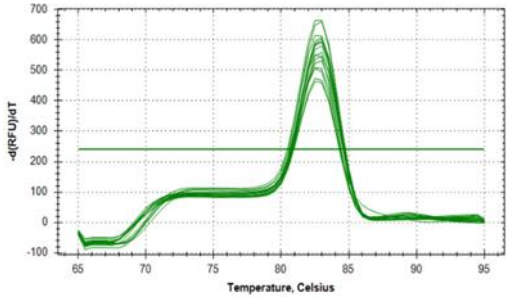

Mki67

E17.5

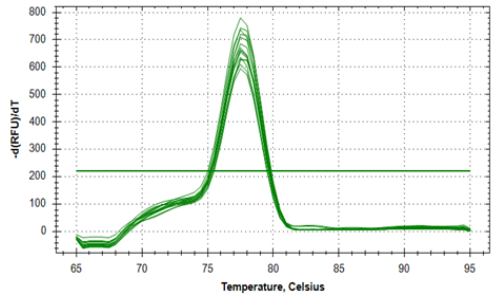

E18.5

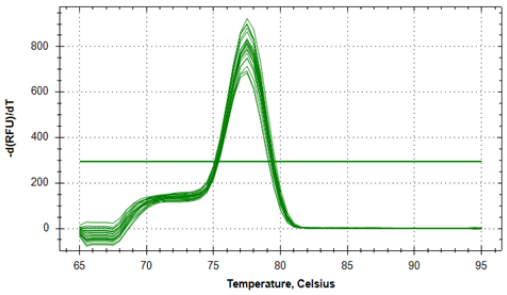

Bcl2

E17.5

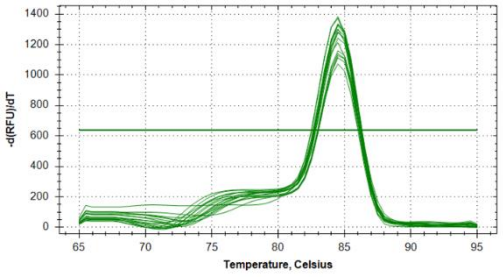

E18.5

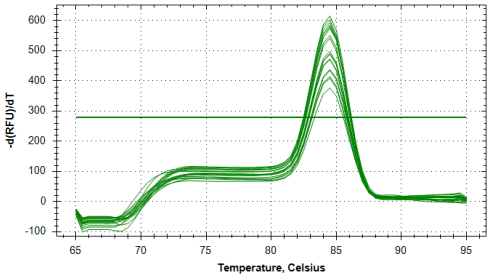

Bax

E17.5

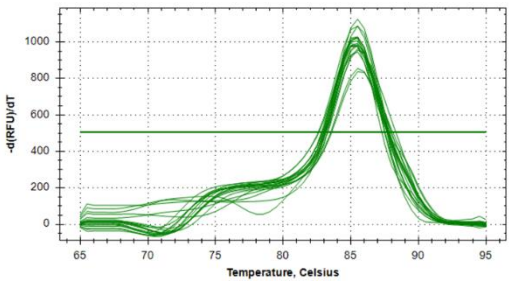

E18.5

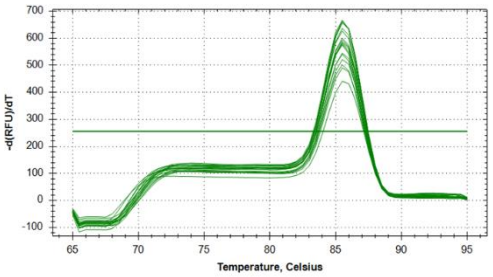

Lamp2a

E18.5

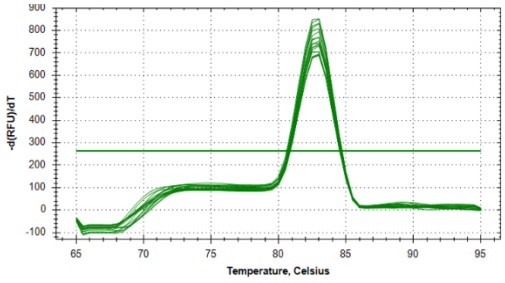

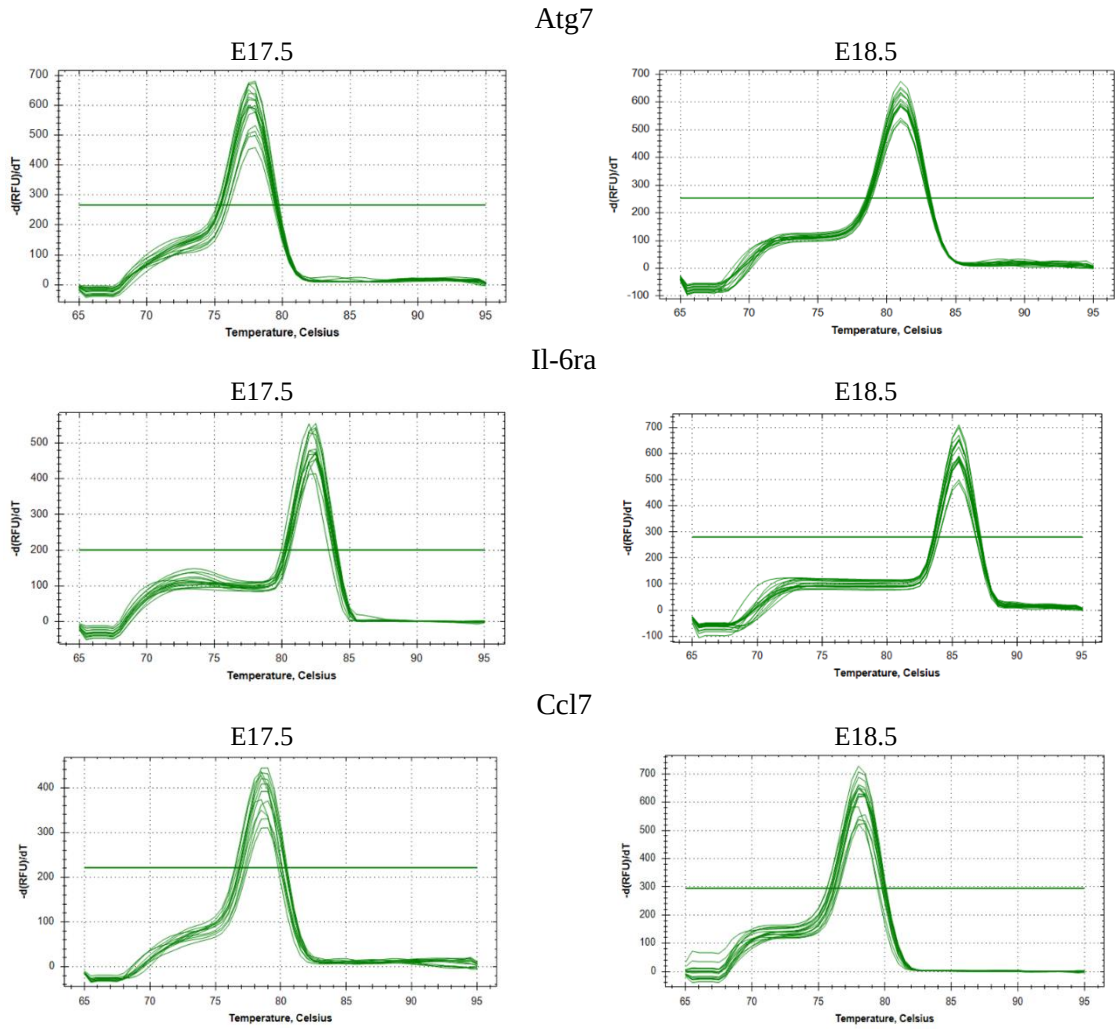

Figure S1 RT-qPCR melting curves, corresponding to each gene (*Cdkn1a*, *Cdkn1c*, *Pim1*, *Mki67*, *Bcl2*, *Bax*, *Lamp2a*, *Atg7*, *Il-6ra*, *Ccl7*) and embryonic stage (E17.5 and E18.5) analyzed shown on figure 3.1.

Table S5 Antibodies used for Western Blot and Immunofluorescence, and respective dilutions.

Antibody	Raised in	Primary vs Secondary	Dilution	Catalog number	Brand
Western Blot					
Histone H3	Rabbit	Primary	1:2000	9715	Cell Signaling
phospho-Histone H3 (Ser10)	Mouse	Primary	1:1000	06-570	Sigma-Aldrich
STAT3	Rabbit	Primary	1:1000	12640	Cell Signaling
pSTAT3	Rabbit	Primary	1:1000	9145	Cell Signaling
p53	Mouse	Primary	1:1000	2524	Cell Signaling
Cdc2 p34	Mouse	Primary	1:1000	sc-54	Santa Cruz
Vinculin	Mouse	Primary	1:1000	ab18058	Abcam
anti-Mouse IgG-HRP	Goat	Secondary	1:5000	AB_10015289	Jackson Immunoresearch Europe

anti-Rabbit IgG-HRP	Goat	Secondary	1:5000	AB_2313567	Jackson Immunoresearch Europe
Immunofluorescence					
phospho-Histone H3	Rabbit	Primary	1:100	06-570	Merk Millipore
anti-Rabbit IgG Alexa 568	-	Secondary	1:1000	A21069	Mol. Probes

Table S6 Guide RNAs (gRNAs) sequences used in CRISPR/Cas9.

Gene	Name	Exon	Sequence	Brand
Lama2	gRNA43	4	5' GGCTGCCTTCACAATTACGT 3'	VectorBuilder
	gRNA167	9	5' GATGAGAAATATGCCCAGCG 3'	
p53	gRNA33	4	5' AACAGATCGTCCATGCAGTG 3'	
	gRNA3	3	5' TGAGGGCTTACCATCACCAT 3'	This work

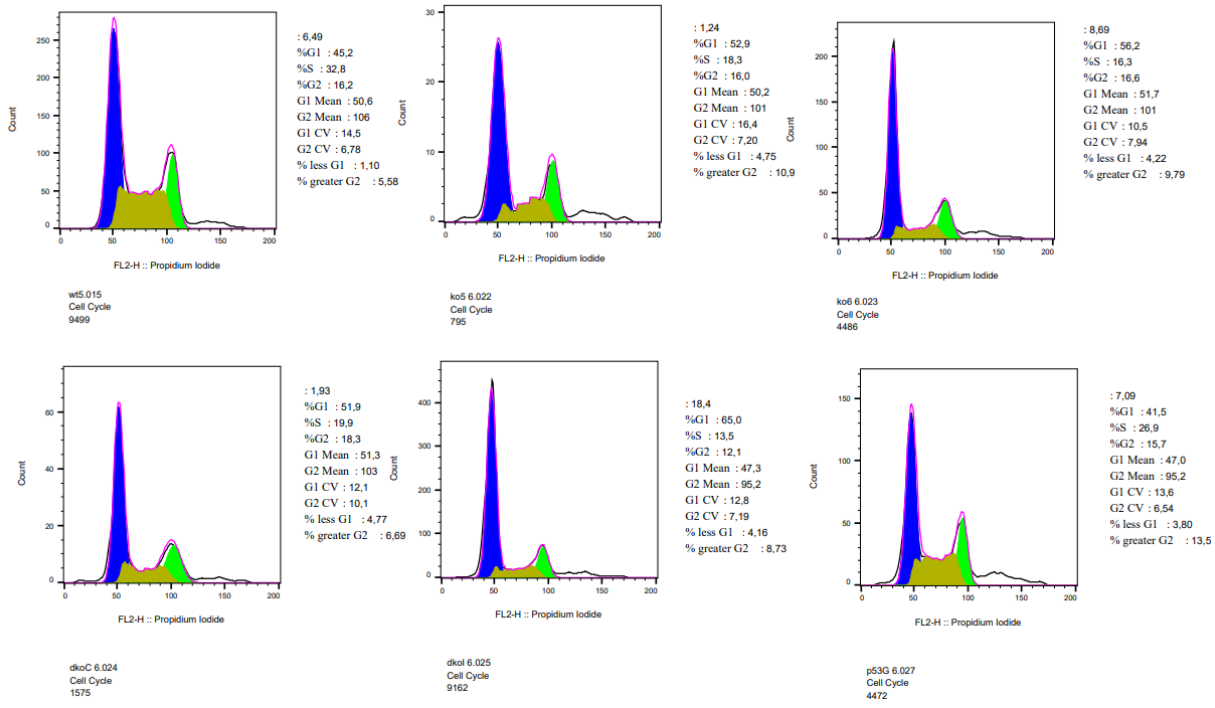

Figure S2 Flow cytometry histograms relative to the cell cycle phase analysis (blue – G1/G0 phase, yellow – S phase and green – G2/M phase), representing an example of each clone – Wt, ko5, ko6, dko C, dko I and p53 D, shown on figure 3.6 D.